

# **Inhibition of glutamine synthetase in monocytes from patients with Acute-on-Chronic Liver Failure resuscitates their antibacterial and inflammatory capacity**

**Short running title:** Reviving monocyte function in ACLF

Hannelie Korf<sup>1,†</sup>, Johannie du Plessis<sup>1,2</sup>, Jos van Pelt<sup>3</sup>, Sofie De Groote<sup>1</sup>, David Cassiman<sup>1,4</sup>, Len Verbeke<sup>1,4</sup>, Bart Ghesquière<sup>5</sup>, Sarah-Maria Fendt<sup>6,7</sup>, Matthew J Bird<sup>1,5</sup>, Ali Talebi<sup>8</sup>, Matthias Van Haele<sup>9</sup>, Rita Feio-Azevedo<sup>1</sup>, Lore Meelberghs<sup>1</sup>, Tania Roskams<sup>9</sup>, Rajeshwar P. Mookerjee<sup>10</sup>, Gautam Mehta<sup>10</sup>, Rajiv Jalan<sup>10</sup>, Thierry Gustot<sup>11</sup>, Wim Laleman<sup>1,4</sup>, Frederik Nevens<sup>1,4</sup>, Schalk van der Merwe<sup>1,4†</sup>

<sup>1</sup>Laboratory of Hepatology, Department of Chronic Diseases, Metabolism and Ageing (CHROMETA), KU Leuven, Belgium

<sup>2</sup>Department of Immunology, University of Pretoria, Pretoria, South Africa

<sup>3</sup>Department of Oncology, KU Leuven, and Leuven Cancer Institute (LKI), Leuven, Belgium

<sup>4</sup>Department of Gastroenterology and Hepatology, UZ Leuven, Leuven, Belgium

<sup>5</sup>Metabolomics Expertise centrum, VIB-KU Leuven Center for Cancer Biology, KU Leuven, Leuven, Belgium

<sup>6</sup>Laboratory of Cellular Metabolism and Metabolic Regulation, VIB-KU Leuven Center for Cancer Biology, KU Leuven, Leuven, Belgium

<sup>7</sup>Laboratory of Cellular Metabolism and Metabolic Regulation, Department of Oncology, KU Leuven and Leuven Cancer Institute (LKI), Leuven, Belgium

<sup>8</sup>Laboratory of Lipid Metabolism and Cancer, Department of Oncology, LKI – Leuven Cancer Institute, KU Leuven, Leuven, Belgium

<sup>9</sup>Department of Imaging and Pathology, Translational Cell and Tissue Research, KU Leuven and University Hospitals Leuven, Leuven, Belgium

<sup>10</sup>Liver Failure Group, Institute for Liver Disease Health, University College London, London, United Kingdom

<sup>11</sup>Erasmus Hospital, Universite Libre de Bruxelles (ULB), Brussels, Belgium

Corresponding authors: Hannelie Korf & Schalk van der Merwe<sup>†</sup>  
([hannelie.korf@kuleuven.be](mailto:hannelie.korf@kuleuven.be); [schalk.vandermerwe@uzleuven.be](mailto:schalk.vandermerwe@uzleuven.be))

This work was supported by internal funding from the UZ Leuven (KOOR) and KU Leuven (C1).

None of the authors have any conflict of interest

**Author contributions:**

SvdM, HK and JvP conceptualized and planned the study

HK, JdP and SvdM wrote the protocol

HK and JdP performed the flow cytometry, monocyte functional studies, gene expression and multiplex cytokine assays

AT, SDG, RFA assisted with the Incucyte experiments

LM documented the clinical patient information

MVH and TR performed immunohistochemistry experiments

BG, DC, MB and SF provided support for the metabolic aspects of the study

JvP performed the RNA sequence pathway identification, the hierarchic clustering and statistical analysis

RJ, GM, RPM, TG, DC, FN, WL, LV and SvdM recruited and cared for the patients

HK and SvdM wrote the manuscript

Abbreviations: ACLF, Acute-on-chronic liver failure; GLUL, glutamine synthetase; GLS, glutaminase; CLIF-SOFA, Consortium on Chronic Liver Failure–Sequential Organ Failure Assessment; PBMC, peripheral blood mononuclear cells; NGS, Next Generation RNAsequencing; UDP-GlcNAc, uridine diphosphate N-acetylglucosamine; MSO, glutamine synthetase, methionine sulfoximine; TCA, tricarboxylic acid; DAMPS, damage-associated molecular patterns; PRKCE, protein kinase C; IRF, Interferon regulatory factor

Word count: 4428 (without title page, abstract, box, references and figure legends)

## **Abstract**

**Objective:** Acute-on-chronic liver failure (ACLF) is associated with dysfunctional circulating monocytes whereby patients become highly susceptible to bacterial infections. Here we identify the pathways underlying monocyte dysfunction in ACLF and investigate whether metabolic rewiring reinstates their phagocytic and inflammatory capacity.

**Design:** Following phenotypic characterization, we performed RNA sequencing on CD14<sup>+</sup>CD16<sup>-</sup> monocytes from ACLF and decompensated alcoholic cirrhosis patients. Additionally, an *in vitro* model mimicking ACLF patient-derived features was implemented to investigate the efficacy of metabolic regulators on monocyte function.

**Results:** Monocytes from ACLF patients featured elevated frequencies of IL-10-producing cells, reduced HLA-DR expression and, impaired phagocytic- and oxidative burst capacity. Transcriptional profiling of isolated CD14<sup>+</sup>CD16<sup>-</sup> monocytes in ACLF revealed upregulation of an array of immunosuppressive parameters and compromised antibacterial- and antigen presentation machinery. In contrast, monocytes in decompensated cirrhosis showed intact capacity to respond to inflammatory triggers. Culturing healthy monocytes in ACLF plasma mimicked the immunosuppressive characteristics observed in patients, inducing a blunted phagocytic response and metabolic program associated with a tolerant state. Metabolic rewiring of the cells using a pharmacological inhibitor of glutamine synthetase, partially restored the phagocytic and inflammatory capacity of *in vitro*-generated- as well as ACLF patient-derived monocytes. Highlighting its biological relevance, the glutamine synthetase/glutaminase ratio of ACLF patient-derived monocytes positively correlated with disease severity scores.

**Conclusion:** In ACLF, monocytes feature a distinct transcriptional profile, polarized towards an immunotolerant state and altered metabolism. We demonstrated that metabolic rewiring of ACLF monocytes partially revives their function, opening up new options for therapeutic targeting in these patients.

## Summary Box

### 1. *What is already known about this subject?*

- Monocyte dysfunction during ACLF is a well-described phenomenon
- Singular factors such as MerTK or prostaglandin E2 have been implicated as potential mechanisms responsible for the suppressive status of monocyte during ACLF syndrome, however the overarching pathways that drive and sustain these disease-associated defects are not fully understood.

### 2. *What are the new findings?*

- Extensive characterization of monocytes from ACLF patients support a transcriptional, functional and metabolic switch towards immunotolerant state.
- The transcriptional signature of ACLF patient-derived monocytes was distinct from that obtained from decompensated cirrhosis patients.
- Feeding glutamine into the TCA cycle by using a pharmacological inhibitor of glutamine synthetase (GLUL), restored the phagocytic and inflammatory capacity of monocytes from ACLF patients.
- Underscoring the biological relevance of this finding, we detected a positive correlation between GLUL/GLS ratio and MELD disease severity scores.

### 3. *How might it impact on clinical practice in the foreseeable future?*

- This study demonstrates that pharmacological regulation of metabolic programs partially restored the dysregulated monocyte function in ACLF.
- These results may open new avenues for the development of therapeutic strategies to restore monocyte function in ACLF.

## **Introduction**

Cirrhosis is the end result of chronic liver disease where persistent inflammation and stellate cell activation leads to collagen deposition, fibrosis, disruption of the intrahepatic venous flow and the development of portal hypertension [1]. Initially, the disease course may be asymptomatic, but if the insult persists, it may progress to decompensated cirrhosis with development of ascites, variceal bleeding and encephalopathy. However, at any moment during the disease course a precipitating event can trigger rapid deterioration of liver function and organ failure, referred to as acute-on-chronic liver failure (ACLF) associated with high in-hospital mortality rates, approaching 70% [2–6]. Importantly, ACLF is often precipitated by bacterial infections, which in turn may initiate a cascade of events resulting in multiple organ failure, irreversible septic shock and death [7,8]. The reason why the immune system in cirrhosis is defective and patients prone to infections is only partly understood. One reason may be that the immune paralysis observed in cirrhosis is the result of exhaustion of circulating innate immune cells such as monocytes by continuous exposure to, and activation by damage-associated molecular patterns (DAMP's) released from the necrotic liver and from bacterial products translocation from the gut [9,10].

Circulating monocytes are central players in the host innate immune defense against invading pathogens since they can interpret the extent of the microbial threat and raise an appropriate inflammatory response to contain the infection [11,12]. Following clearance, it is equally important that regulatory mechanisms are initiated to counteract excessive inflammation. Macrophages for instance are known for their plasticity in adopting either an inflammatory- or regulatory phenotype [13–15]. During the course of ACLF however, it is unclear whether patients succumb to infection due to a failure of monocytes/macrophages to sufficiently dampen the production of pro-inflammatory mediators leading to septic shock and organ damage, or whether they trigger a prolonged anti-inflammatory response rendering the patient incapable to respond to secondary infections. Nevertheless, studies taking a snap-shot of ACLF monocyte function at a given time, have confirmed the presence of a suppressive monocyte phenotype with reduced HLA-DR surface expression, antigen presentation capacity as well as impaired ability to secrete pro-inflammatory cytokines in response to bacterial components [16–19]. Although singular factors such as MerTK or prostaglandin E2 have been implicated as potential mechanisms responsible for monocyte dysfunction during ACLF syndrome [18,19], the overarching pathways that drive and sustain these disease-associated defects are not fully understood.

The functional phenotype of monocytes/macrophages is highly regulated at both transcriptional and metabolic levels [20,21]. To exert their immunological functions, they can metabolize a variety of carbon substrates [22,23], and the nature of the metabolic program involved is critically associated with their activation status [24–26]. For example, pro-inflammatory macrophages consume glucose and heavily rely on glycolysis for ATP generation. Additionally, they exhibit a “broken” tricarboxylic acid (TCA) cycle, allowing accumulation of citrate and succinate. On the other hand, anti-inflammatory monocytes/macrophages maintain an intact TCA cycle and favor fatty acid oxidation, as a mode of ATP production [26–28]. In this study, the aim was to obtain a comprehensive view of the transcriptional profile of monocytes from ACLF patients and to investigate whether their molecular signature correlated with a functional and metabolic switch towards a suppressive phenotype. More importantly, we investigated whether metabolic rewiring of the cells using pharmacological inhibitors that channel glutamine into the TCA cycle, could restore ACLF monocyte dysfunction. These results may provide new insights into fundamental disease mechanisms.

## **Materials and methods**

### **Patient characteristics**

For this study we recruited healthy controls, decompensated alcoholic cirrhosis, and ACLF patients diagnosed at the University hospital of Leuven between July 2013 to May 2017. Patients with alcoholic liver disease were identified and prospectively included at first contact in the emergency room (ER), the liver ward or the medical intensive care unit. Patients that used antibiotics or corticosteroid therapy during the 6 weeks preceding admission were not considered for inclusion in the study. Patients with concomitant other liver diseases including viral hepatitis were excluded from participation. Blood was collected for study purposes before initiating other therapy. Blood and urine cultures were obtained, ascites fluid collected for analysis and a chest X-rays performed to exclude infections and pulmonary infiltrates as per standard of care. Patients with ACLF were classified according to the Consortium on Chronic Liver Failure–Sequential Organ Failure Assessment [CLIF-SOFA] classification [4]. Written informed consent was obtained from all patients or their designated family members and the study protocols were approved by the Ethical Commission UZ / KU Leuven (S54588).

### **Plasma cytokine measurements**

Custom Meso Scale Discovery V-plex assays (Gaithersburg, MD) were used to determine plasma cytokine (IL-6, IL-8, IL-10 and TNF $\alpha$  and chemokine (CCL2 and CCL3) levels. All measurements were performed in duplicate according to manufactures instructions.

### **Phenotypic analysis of monocyte subsets and intracellular cytokine determination**

Peripheral blood mononuclear cells (PBMCs) were isolated and stained with the following antibodies: CD3, CD19, CD56, CD14, CD16, HLA-DR (eBioscience, San Diego, CA) and matching isotype controls. Flow cytometric data acquisition was performed on a Gallios flow cytometer (Beckman Coulter, Analis, Belgium) and analyzed using FlowJo software [29]. For intracellular staining, PBMCs were stimulated with LPS and brefeldin A (eBioscience), for 18 h and then stained with the same surface antibody cocktail as described above followed by the addition of Cytofix/Cytoperm (eBioscience) and anti-human IL-10 (BD Biosciences, Erembodegem, Belgium).

### **Monocyte isolation and culture**

Blood was collected from healthy donors and ACLF patients in heparin-coated tubes (BD Biosciences). Immediately after collection, CD14<sup>+</sup> monocytes were isolated from the PBMC

fraction using a negative selection procedure according to the manufacturer's specifications (Dynabeads untouched human monocyte kit, Invitrogen, Lennik, Belgium). Monocytes were cultured in RPMI medium containing antibiotics and further supplemented either with plasma from healthy donors or plasma from ACLF patients to give a final concentration of 20% by volume. Patient plasma used in these experiments represent a pool of 4 donors with ACLF grade 2. Plasma was heat-inactivated (56°C for 30 min) and passed through a 0,22 µM filter prior to use. Following a 16-hour incubation time (37°C, 5 % CO<sub>2</sub>), the cells were harvested for transcriptional analysis or functional assessment of their phagocytic capacity as described below.

### **Monocyte phagocytic- and oxidative burst capacity following exposure to *E. coli***

The phagocytic and oxidative burst capacity of human monocytes were assessed as previously described [30]. Briefly, 100 µl heparinized peripheral blood was incubated for 1 hour at 37°C with pH-rodoRed-labeled *E. coli* bacteria (Invitrogen), previously opsonized with *E. coli* BioParticles®opsonizing reagent (Invitrogen). This was followed by the addition of the fluorogenic substrate rhodamine (20 min at 37°C) and staining for human monocyte markers. Flow cytometric data acquisition was performed as described above.

### **RNA isolation and RNA-sequencing analysis**

RNA was isolated from freshly isolated monocytes, and from monocytes cultured in the presence or absence of ACLF plasma for 12 hours. RNA quantity and quality was measured, and samples meeting RNA integrity criteria were used for NextGeneration RNA-Sequencing (NGS) analysis using Illumina NextSeq instrument (detailed description in supplements). Sequencing and initial processing of the raw data was performed by the Nucleomics Core Facility, VIB, Leuven. Sequencing data are available at the Gene Expression Omnibus (<http://www.ncbi.nlm.nih.gov/geo/>) under accession number GSE93265.

### **Data analysis**

After preprocessing, reads were aligned to the reference genome of Homo sapiens (GRCh37.73) and a generalized linear model was fitted (described in supplements). Two types of analysis were performed: 1) Unpaired analysis between CD14<sup>+</sup> monocytes from ACLF patient's vs healthy controls (reflecting the *ex vivo* transcriptional profile) and 2) Paired analysis of CD14<sup>+</sup> monocytes cultured in the presence or absence of ACLF plasma for 12 hours (reflecting an *in vitro* simulation of acute ACLF). The individual results were combined, the average calculated

and the resulting p-values were computed. A gene was considered differentially expressed if a 2log fold change  $>+1$  or  $<-1$  and a corrected  $p < 0.05$  (see supplemental text for more detail). The genes differentially expressed in the same direction within both *ex vivo* ACLF patient samples as well as *in vitro* following monocyte exposure to ACLF plasma were used as input in the software packet Webgestalt (<http://www.webgestalt.org>). As read-out we analysed GO:Biological Processes (<http://geneontology.org/>), to explore the *ex vivo* patient samples. Alternatively, KEGG Pathways was used to explore the pathways involved following *in vitro* exposure of CD14<sup>+</sup> monocytes to ACLF serum, (<http://www.genome.jp/kegg/pathway.html>).

### **Live-cell real-time phagocytosis assay**

Isolated CD14<sup>+</sup>CD16<sup>-</sup> monocytes were plated onto 96-well clear flat-bottom polystyrene tissue-culture treated microplates and allowed to adhere. Monocytes were cultured in RPMI 1640 medium containing antibiotics and further supplemented either with plasma from healthy donors or plasma from ACLF patients at a final concentration of 20% by volume (see above). In some instances the cells were treated with Methionine sulfoximine at the indicated concentrations. pHrodo® pathogen bioparticles were added at indicated concentrations and the plates were transferred into a humidified incubator (37°C, 5%, CO<sub>2</sub>) and measured in real time using an IncuCyte Zoom imager (Satorius). Four images per well from three technical replicates were taken every 2 hours using a 10× objective lens and then analyzed using the IncuCyte™ Basic Software.

### **Real-Time qPCR**

cDNA was synthesized using SuperScript II reverse transcriptase and random hexamer primers (Invitrogen/Life Technologies, USA). The PCR reaction was carried out in a mixture that contained appropriate sense- and anti-sense primers and a TaqMan MGB probe in Taq-Man Universal PCR Master Mixture (Applied Biosystems, Foster City, USA). Beta-2-microglobulin was used as housekeeping gene. qRT-PCR amplification and data analysis were performed using the Lightcycler 96 (Roche Applied Science, Penzberg, Germany). Each sample was assayed in duplicate. The  $\Delta\Delta C_q$  method was used to determine relative gene expression levels.

### **Statistical analysis**

Group comparisons were performed using Kruskal-Wallis with Dunn's correction for multiple testing or Mann-Whitney-Wilcoxon rank sum tests where appropriate. Spearman correlation was used to determine associations between variables. Statistical analyses were performed

using JMP® version 11.0.0 (SAS Institute, Inc, Cary, NC) and SigmaPlot 12.0 (Systat Software, Inc., San Jose, USA). Two-sided P-value < 0.05 was considered statistical significant.

## **Results**

### **ACLF monocyte subset distribution, phenotype and cytokine response differ from decompensated cirrhosis patients**

Patients with ACLF are highly susceptible to infections and monocytes represent the first line of defense against pathogens entering the systemic circulation. Failure of monocytes to respond to danger signals may be due to an over production of immunosuppressive factors and/or the induction of a tolerant state. To identify the mechanisms that play a role in monocyte dysfunction during ACLF, we evaluated the expression of characteristic immunosuppressive markers such as intracellular IL-10 or surface expression of HLA-DR as read-out for their antigen presentation capacity. We specifically investigated whether these features from ACLF monocytes were different from those observed in decompensated cirrhosis patients. The clinical characteristics as well as circulating biochemical and immunological parameters of the patient cohort are documented in Supplemental Table 1 and Supplemental Figure 1. Flow cytometric analysis of monocyte distribution showed a significant decrease in the classical monocyte subset and expansion of the intermediate monocyte population (Figure 1A). Further, indicative of a decreased activation status, all monocyte subsets expressed lower levels of surface HLA-DR. The latter observation was most pronounced in monocytes from ACLF patients (Figure 1B). Additionally, we assayed intracellular IL-10 production following LPS exposure and detected elevated numbers of IL-10 producing monocytes within the intermediate monocyte as well as the classical monocyte subsets from ACLF patients, suggesting an elevated immunosuppressive function (Figure 1C).

### **ACLF monocytes feature a distinctive immunosuppressive transcriptional profile**

To obtain an in-depth understanding of the molecular signatures responsible for this dysfunctional response, we performed a transcriptomic analysis of classical monocytes as the most abundant monocyte subset. CD14<sup>+</sup> cells from ACLF patients (n=9), -decompensated cirrhosis patients (n=4) and -healthy controls (n=5) were freshly isolated with a negative selection strategy whereby CD16<sup>+</sup> cells were additionally depleted along with all other unwanted cell types to avoid granulocyte contamination (see materials and methods for full description). Notably, ACLF grade 2 patients were included for this purpose to ensure homogeneity within this experimental group whereby the disease status can be very dynamic (see supplemental Table 2 for patient characteristics). Gene Ontology analysis to assess the biological processes involved revealed that the up-regulated genes from decompensated cirrhosis monocytes predominantly associated with immune response or leukocyte activation

(Figure 2A). Conversely, biological pathways promoting immunological processes and cell activation were associated with the down-regulated genes in ACLF patient monocytes (Figure 2B). Although there was an overlap of differentially regulated genes between these two conditions (not shown), the comparison of ACLF monocyte profiles to that of decompensated cirrhosis patients, unveiled unique differences of ACLF as disease entity. In this regard, the immunosuppressive nature in ACLF is further highlighted since the majority of the down regulated genes involve immune response processes (Figure 2C).

Focusing specifically on subsets of immune-related genes illustrated that patient- as well as healthy monocytes cluster together, indicative of their distinct gene expression profiles. Heat maps of markers characteristically expressed by pro-inflammatory monocytes/macrophages (M1-like) were predominantly repressed (Figure 2D). These include cytokines and their receptors (*TNFa*, *IL15*, *IL15R*, *IL23A*, *IL1B*), chemokines (*CCL4*, *CXCL9*, *CXCL10*), co-stimulators of antigen presentation (*CD80*, *CD83*) as well as transcription factors (*STAT1*). In sharp contrast, anti-inflammatory markers (M2-like) were largely overexpressed in monocytes from ACLF patients (Figure 2E). We observed a number of scavenger receptors (*CD163*, *MRC1*, *CD36*, *MARCO*), growth factors (*HGF*), suppressive cytokines (*IL10*), chemokines (*CCL22*) as well molecules involved in phagocytosis of apoptotic cells (*MERTK*, *TGM2*) and markers M2-like surface phenotype (*MS4A4A*) to be upregulated. In line with previous reports [31,32], we detected an increased frequency of MerTK-positive cells with a macrophage-like morphology in the liver tissue ACLF- compared to decompensated patients (Supplemental Figure 3). Furthermore, ACLF monocytes featured dampened expression of a battery of antigen presentation molecules (*HLA*), as well as co-activator (*CIITA*), molecular scaffold (*TAP2*) and molecules needed for proper folding and trafficking of MHC class II (*CD74*) (Supplemental Figure 2). Conversely, a number of heat-shock proteins (*HSPA1A*, *HSPA1B*, *HSPA1L*, *HSPA6*) which act as chaperones for proper folding and transport of newly synthesized polypeptides, were specifically upregulated within ACLF monocytes (Supplemental Figure 2). Combined, our data reveal that the extent of the immunosuppressive status of ACLF monocytes goes beyond what has been documented before and implicate major defects in their potential to mount pro-inflammatory responses and raise T-cell reactivity against pathogens (Figure 1B).

### **Defective antibacterial response of ACLF monocytes**

We next aimed to evaluate whether immune dysfunction in ACLF translates into a defective functional capacity of monocytes to detect, engulf and respond to infection. To investigate

monocyte ability to detect and recognize bacteria, we evaluated basal surface expression of both TLR2 and TLR4 on classical monocytes from the different patient groups. Interestingly, both decompensated cirrhosis patients as well as ACLF patients portrayed dampened expression levels of these markers (Figure 3A & 3B). We further assessed the *ex vivo* phagocytic and oxidative burst capacity of these cells following exposure to *E. coli*. In line with defective bacterial recognition, monocytes isolated from both decompensated as well as ACLF patients featured a significantly impaired phagocytic capacity, although this defect was most prominent in patients with ACLF (Figure 3C). Monocytes from ACLF patients also featured a clear defective oxidative burst response, following interaction with *E.coli* (Figure 3D). To further identify the underlying pathways leading to this functional defect we investigated differentially regulated genes related to the antibacterial and oxidative burst response of monocytes originating from ACLF patients (see schematic representation of the components involved within Figure 3E). Notably, we detected dampened expression of IRF8, a prominent regulator of monocyte/macrophage pro-inflammatory- and anti-bacterial function. Dampened expression levels of IRF8 may implicate a defective ability to activate transcription of constituents of the NADPH oxidase complex, a key component of the oxidative burst response [33]. Nevertheless, the activity of the subunits within the NADPH oxidase complex can be regulated in different ways including at the level of post-translational modification. In this regard, we observed significantly lower levels of protein kinase C (PRKCE) within ACLF monocytes, suggesting that the defective oxidative burst may be partially related to inadequate phosphorylation of NADPH oxidase subunits. Furthermore, we detected the upregulation of Rnf145, a E3 ubiquitin ligase that negatively regulates gp91phox steady-state protein levels. Combined, our data highlight a number of mechanisms that may explain the functional defect of ACLF patients to respond to- and eradicate infections.

### **Monocytes cultured with ACLF plasma mimic functional and transcriptional disease characteristics**

In order to explore the possibilities of reversing monocyte dysfunction, we devised an ACLF disease-mimicking *in vitro* model whereby freshly isolated CD14<sup>+</sup> monocytes from healthy donors were cultured for 16 hours either in the presence of pooled plasma (20% v/v) from ACLF grade 2 patients or normal human plasma (Figure 4A). We first evaluated whether freshly isolated healthy CD14<sup>+</sup> monocytes exposed to pooled ACLF grade 2 plasma *in vitro*, exhibit a transcriptional profile similar to that observed in monocytes obtained from ACLF patients. Indeed, the transcriptional signature obtained mimicked that of monocytes obtained from ACLF

patients, showing a clear elevation of anti-inflammatory (M2-like), but only a partial dampening of inflammatory (M1-like) markers at 16 hours after exposure (Illustrated by the heat maps within Figure 4B & C). In line with the previous data, qPCR- and multiplex immune assay showed that ACLF plasma triggered a clear induction of anti-inflammatory parameters (IL-10 and/or MerTK) while a tendency to dampen pro-inflammatory mediators (TNF $\alpha$ , IL-8) was observed in cultured monocytes (Figure 4D, E, F & G). Finally, to verify whether ACLF plasma-conditioned monocytes also portrayed a defective phagocytic activity we evaluated their ability to engulf gram-negative pHrodo-labeled *E.coli* particles over time using the IncuCyte Zoom system. The data indicate that ACLF plasma blunted the phagocytic capacity of healthy donor-derived monocytes (Figure 4H). Of note, this defect in bacterial uptake only became apparent after 8-16 hours following conditioning of the cells in ACLF plasma. Interestingly monocytes cultured in the presence of ACLF plasma featured a similar defective capacity to engulf gram-positive pHrodo-labeled *S. aureus* particles (Supplementary Figure 4). Combined, this observation strongly supports the hypothesis that circulating plasma derived factor(s) in ACLF plasma induce an ACLF-like phenotype in healthy donor derived monocytes.

### **Metabolic rewiring and promoting TCA cycle metabolism, restores the phagocytic capacity of *in vitro* generated- as well as monocytes from ACLF patients**

Mounting evidence suggests that immune-suppressive cells exhibit unique metabolic requirements [33,34]. In particular, they maintain an intact TCA cycle and favor oxidative metabolism, especially fatty acid oxidation, as a mode of ATP production. Similar to what has been described for M2 macrophages, ACLF-conditioned monocytes also featured low glycolysis activity with lower expression of glycolytic enzymes (*HK1*, *PGK1*, *PFKM*, *ENO2*) (Figure 5A & Supplemental Figure 5). Glutamine, on the other hand can be catabolized thereby fueling the TCA cycle (Fig. 5A) [35]. We next argued that continued glutamine anabolism through glutamine synthetase (GLUL) may be responsible for the sustained suppressive phenotype of ACLF monocytes and we therefore implemented a strategy to redirect glutamine into the TCA cycle by inhibiting its enzyme activity. Hereto we tested the ability of the inhibitor of glutamine synthetase, methionine sulfoximine (MSO), to restore the phagocytic capacity of ACLF-plasma-conditioned monocytes (the concept thereof can be visualized in Figure 5B). Strikingly, treatment of monocytes cultured in the presence of ACLF plasma with MSO triggered a dose-dependent increase in their ability to phagocytose *E. coli* bioparticles (Figure 5C). Considering the importance of the above findings, we reanalyzed the expression levels of parameters involved in glutamine metabolism within ACLF patient monocytes. More

specifically, we calculated the ratio of glutamine anabolism over catabolism by assessing GLUL and GLS1 expression levels. Interestingly, the data clearly indicate an elevated GLUL/GLS ratio for monocyte originating from ACLF patients compared to healthy counterparts (Figure 5D). To improve our understanding of the significance of these findings, we investigated possible correlations of the GLUL/GLS ratio with survival or MELD scores of the patients. Importantly our data show that the GLUL/GLS ratio positively correlated with disease severity in ACLF patients (Figure 5E). Treatment of ACLF patient-derived monocytes with MSO similarly improved their capacity to recognize and engulf bacteria (Figure 5F). Finally, treatment of patient monocytes with MSO inhibited IL-10 production while promoting the production of the pro-inflammatory cytokine, TNF $\alpha$  (Figure 5G & H).

## Discussion

Bacterial infection is one of the most common precipitating events in ACLF that may initiate multi-organ failure. The mechanisms and pathways responsible for failure of the host innate immune system to respond to bacterial infections in ACLF are only partly understood. Here we demonstrate that monocytes from ACLF patients show a broad range of innate immune defects, which extend beyond what has been previously documented. This monocyte immunosuppressive signature in ACLF is clearly different from decompensated cirrhosis supporting ACLF as a distinct clinical entity. We further demonstrate the importance of metabolic rewiring in establishing the monocyte phenotype in ACLF and showed that promoting glutamine fuelled TCA cycle metabolism within monocytes, improved their defective phagocytic and inflammatory function.

In our study we observed that ACLF monocytes displayed profound defects in *ex vivo* phagocytic and oxidative burst capacity following exposure to *E. coli* (Fig 3E) that could be recapitulated by exposing healthy monocytes to ACLF plasma (Fig 4G) suggesting a specific defect in anti-bacterial function. We specifically focused on constituents of the Nox2 NADPH oxidase complex, which mediates the generation of reactive oxygen species to kill invading pathogens. Interestingly, although transcription of constituents of the Nox2 NADPH complex were not severely affected, we observed the upregulation of Rnf145, a negative regulator of the Nox2 complex. Rnf145 has recently been implicated in the proteostasis of the Nox2 complex by endoplasmic reticulum-associated degradation [36]. Graham *et al.*, very elegantly demonstrated the importance of this factor as negative regulator by showing that ablation of *Rnf145* in murine macrophages enhance bacterial clearance and rescued the oxidative burst defects associated with *Ncf4* haplo-insufficiency [36]. A further important observation was that ACLF monocytes featured a dampened expression of IRF8, a transcriptional activator of the oxidative burst response. IRF8 along with IRF1 and their downstream targets have been shown to be specifically required for the protection against infection [37]. In addition, IRF8 plays a critical role in monocyte/macrophage polarization to an inflammatory phenotype and as regulator of genes involved in antigen presentation and T cell activation [37,38]. Interestingly, the impaired IRF8 expression within ACLF monocytes was associated with lower levels of molecules involved in antigen presentation- (*HLA*, *CD74*) and T cell co-stimulation (*CD80*, *CD86*) as well as characteristic markers for classically activated immunostimulatory or proinflammatory - M1 monocytes/macrophages (*CXCL9*, *CXCL10*, *IL-15* and *ITGAL*). It is therefore tempting to speculate that an IRF8-dependent mechanism maybe involved in the

failure of ACLF monocytes to raise an appropriate oxidative burst- and inflammatory response. However, besides hampered pro-inflammatory and anti-bacterial defence mechanisms, ACLF monocytes also exhibited elevated expression of markers associated with alternatively activated anti-inflammatory/tolerogenic M2 macrophages including *IL10*, *MERTK*, *CCL22*, *ILAR*, *CD36*, *MARCO* and *CD163*. This result is in line with previous studies showing upregulation of singular anti-inflammatory parameters in monocytes from ACLF patients [18,19]. Combined, our data outline the extent of immune dysfunction within ACLF monocytes and provides possible insights in the underlying mechanism governing the susceptibility to infections, as a characteristic precipitating event during this syndrome.

Interestingly, similar immunosuppressive features along with metabolic- and epigenetic reprogramming have been observed in circulating monocytes from late stage sepsis patients [39,40]. This is in sharp contrast to the characteristic overt upregulation of pro-inflammatory parameters during acute stages of sepsis that resembled more the expression pattern observed in monocytes from decompensated cirrhosis patients [41]. Considering the fact that sepsis is a major cause of death in ACLF patients, future investigations aimed at understanding the mechanisms underlying immune dysfunction, as well as similarities between sepsis-induced- and ACLF-induced immunosuppression, may improve therapeutic strategies [42]. Another potential interesting and important line of investigation is how the source of infection may affect circulating- and peripheral innate immune cells. Intestinal barrier failure and bacterial translocation through the portal vein has recently been shown to directly affect liver residing myeloid cells rendering them incapable of clearing infection [44,45]. It will therefore be intriguing to determine how ACLF monocyte function correlates with the presence of bacteria or its components in the circulation as well as with clinical patient data regarding past and ongoing infections.

Monocyte/macrophage function is not only controlled at the transcriptional- and posttranscriptional level but their metabolic program can also govern their phenotype [33,46]. In particular M2 macrophages maintain an intact TCA cycle and favour oxidative metabolism, especially fatty acid oxidation, as mode of ATP production. Additionally, glutamine anabolism is particularly elevated in M2 macrophages for the generation of UDP-GlcNAc and glycosylation of many characteristic scavenger receptor markers [35,47]. We demonstrate here for the first time that monocytes conditioned with ACLF plasma portrayed a clear downregulation of key parameters in the glycolytic pathway (including *PFKM*, *PGK1* and

*ENO2*) as well as modulation of parameters involved in fatty acid metabolism. Strikingly, blocking glutamine synthetase using an inhibitor thereof improved the capacity to clear bacteria both in ACLF-plasma conditioned monocytes as well as monocytes derived from ACLF patients. Furthermore, we demonstrate that monocytes derived from ACLF patients feature elevated expression of enzymes regulating glutamine anabolism (GLUL) and dampened expression of enzymes regulating glutamine catabolism (GLS). Underscoring the biological relevance of this finding, we detected a positive correlation between GLUL/GLS ratio and MELD disease severity scores. Interestingly, in the cancer research field such metabolic rewiring of tumour-associated macrophages, through the inhibition of glutamine synthetase, has been shown to revert M2 macrophages towards an M1-like phenotype, that promoted immunostimulatory and antiangiogenic effects that prevented the development of metastasis [48]. Our results are in line with these findings showing decreased IL-10 and elevated TNF $\alpha$  production by patient monocytes following inhibition of glutamine synthetase. Glutamine synthetase therefore may represent an important checkpoint in the regulation of the immunological function of monocytes/macrophages both in cancer as well as in response to bacterial infections.

In addition to characterizing the full extent of innate immune dysfunction of monocytes from ACLF patients, we highlight a number of possible mechanisms that may explain increased susceptibility to infections. Our data also demonstrates that metabolic programs can be manipulated to rescue defective monocyte phagocytic functions. Finally, this work highlights the importance of metabolic immunotherapeutic strategies in the treatment of ACLF and it will be intriguing for future work to further fine-tune and develop this approach as potential interventional strategy.

## **Acknowledgments**

Schalk van der Merwe, Frederik Nevens and David Cassiman are recipients of Flanders fund for scientific research (FWO fundamenteel-klinisch mandaat). The authors wish to acknowledge the contributions of the VIB-Nucleomics Core for excellent assistance in the RNA sequencing experiments. We also wish to thank Petra Windmolders, Ingrid Vander Elst and Elien de Smidt for the excellent technical assistance.

## Figure legends

**Figure 1. Phenotypic and functional analysis of monocyte subsets within patients with decompensated cirrhosis or ACLF.** Peripheral blood mononuclear cells (PBMCs) were isolated and stained for monocyte specific surface markers. A) Flow cytometric analysis of classical-, intermediate- and non-classical monocyte frequencies in patients with ACLF (n=15), decompensated cirrhosis (Decomp) (n=7) and healthy controls (n=10) (Mean  $\pm$  SEM; \* p<0.05; \*\*p<0.01). B) The quantitative median fluorescence intensity (MFI) of HLA-DR surface expression on classical-, intermediate- and non-classical monocytes obtained from ACLF (n=15), Decomp (n=7) and healthy controls (n=10) (mean  $\pm$  SEM) (\* p<0.05; \*\* p<0.01 compared to controls). C) Frequency of intracellular IL-10-positive classical-, intermediate- and non-classical monocytes in patients with ACLF (n=4), Decomp (n=4) and healthy controls (n=12). The data show mean  $\pm$  SEM (\*, p<0.05).

**Figure 2. Immunosuppressive transcriptional profile of monocytes from ACLF patients.** RNAsequencing was performed on isolated monocytes from ACLF patients (n = 9), decompensated cirrhosis patients (Decomp) (n = 4) and healthy controls (n = 5). Differentially expressed genes with a 2log fold change > +1 or < -1 and FDR< 0.05 were computed to explore patient subgroups. Volcano plots indicate all the up- (red) and downregulated (green) genes within monocytes from Decomp compared to controls (A) or ACLF patients compared to controls (B). Panel C depicts the comparison of ACLF patients versus Decomp. In addition, the top 10 biological processes for the differentially expressed genes were identified and these are indicated as circular charts surrounding the volcano plots. The biological processes that were upregulated are illustrated in a red color on the right side of the volcano plots while the downregulated processes are depicted in a green color to the left of the volcano plots. The size of the circle charts correlates with the number of genes per process that were regulated (the number thereof is indicated in the middle of the chart). The color intensity of the circle charts indicates the significance whereby a biological process were upregulated (dark red = most significant) or downregulated (dark green = most significant). Heat maps of proinflammatory M1 markers (E) or anti-inflammatory M2 markers (E) selected from the RNAseq data shows the close clustering of the monocyte samples within each experimental group. Scale of gene expression is indicated by color ranging from low (green) to high (red).

**Figure 3. Defective antibacterial mechanisms of monocytes from ACLF patients.** Flow cytometric analysis of TLR2 (A) and TLR 4 (B) expression on the surface of CD14<sup>+</sup>CD16<sup>-</sup> monocytes. Flow cytometry data derived from a whole blood phagocytosis and oxidative burst assay following *E. coli* challenge and surface staining for monocyte specific surface markers in patients with ACLF (n=13), -decompensated cirrhosis (Decomp) (n=12) and healthy controls (n=15). Graphs show the percentage of CD14<sup>+</sup>CD16<sup>-</sup> classical monocytes that have internalized *E. coli* bacteria (C) or have produced reactive oxygen species (D). (mean ± SEM; \*p<0.05, \*\*p<0.01, \*\*\*p<0.001). Panel E depicts a schematic representation of components involved in monocyte oxidative burst response. The figure indicates potential checkpoints in the activation or regulation of events in this pathway. Expression levels of *IRF8* (F), *PRKCE* (G), *RNF145* (H) within monocytes from ACLF patients (n = 8), decompensated cirrhosis patients (Decomp) (n = 4) or healthy controls (n = 5) (mean ± SEM; \*p<0.05).

**Figure 4: *In vitro* model to mimic monocyte dysfunction in ACLF.** Freshly isolated CD14<sup>+</sup>CD16<sup>-</sup> monocytes from healthy donors were cultured in the presence of normal human plasma or ACLF patient plasma (20% v/v) (A). RNAsequencing was performed after a culture period of 16 hours to identify differentially expressed genes. Hierarchic clustering of monocytes following conditioning with ACLF plasma (ACLF) or normal human plasma (Normal) was performed using the expression of a subset of proinflammatory M1 (Panel B)- and anti-inflammatory M2 (Panel C) genes. The scale is indicated by a color ranging from low (green) to high (red). Quantification of pro- and anti-inflammatory parameters from monocytes of healthy donors following condition with Normal or ACLF plasma for 16 hours. Relative mRNA levels of pro- (D) or anti-inflammatory parameters (E), were determined by means of RT-qPCR at the end of the culture period (Mean ± SEM; n = 6). Similarly, protein levels of a selection of pro- (F) and anti-inflammatory (G) markers were determined after 16 hours of culture with a high-sensitive multiplex immunoassay. Finally, healthy monocytes were cultured in the presence of ACLF or normal plasma (20% v/v) and challenged with low doses pHrodo-labeled *E.coli* to measure engulfment with the IncuCyte system over a period of 24 hours (H).

**Figure 5. Metabolic reprogramming of ACLF monocytes.** Schematic representation of glucose and glutamine metabolism programs (A). Blocking glutamine synthetase with the

pharmacological inhibitor, methionine sulfoximine (MSO) fuels the TCA cycle (schematic representation) (B). The effect of (MSO) on healthy monocyte's ability to phagocytose bacteria under normal plasma or ACLF plasma conditioning. Monocytes were cultured in the presence of ACLF or normal plasma (20% v/v) and treated with MSO (2mM). Low doses of pHrodo-labeled *E.coli* was added to the cells and engulfment was measured with the IncuCyte system. The results depict the number of pHrodo-positive monocytes over time (C). The GLUL/GLS ratio in monocytes from patients with ACLF compared to monocytes from healthy controls (D). The correlation of GLUL/GLS ratio with the MELD scores of patients with ACLF (E). Monocytes obtained ACLF patient were treated with or without MSO and challenged with low doses of pHrodo-labeled *E.coli* before measuring engulfment with the IncuCyte system (F). Monocytes obtained from ACLF patients were treated with or without MSO and cultured under normal conditions for 16 hours before assessment of IL-10 (G) and TNF $\alpha$  (H) production.

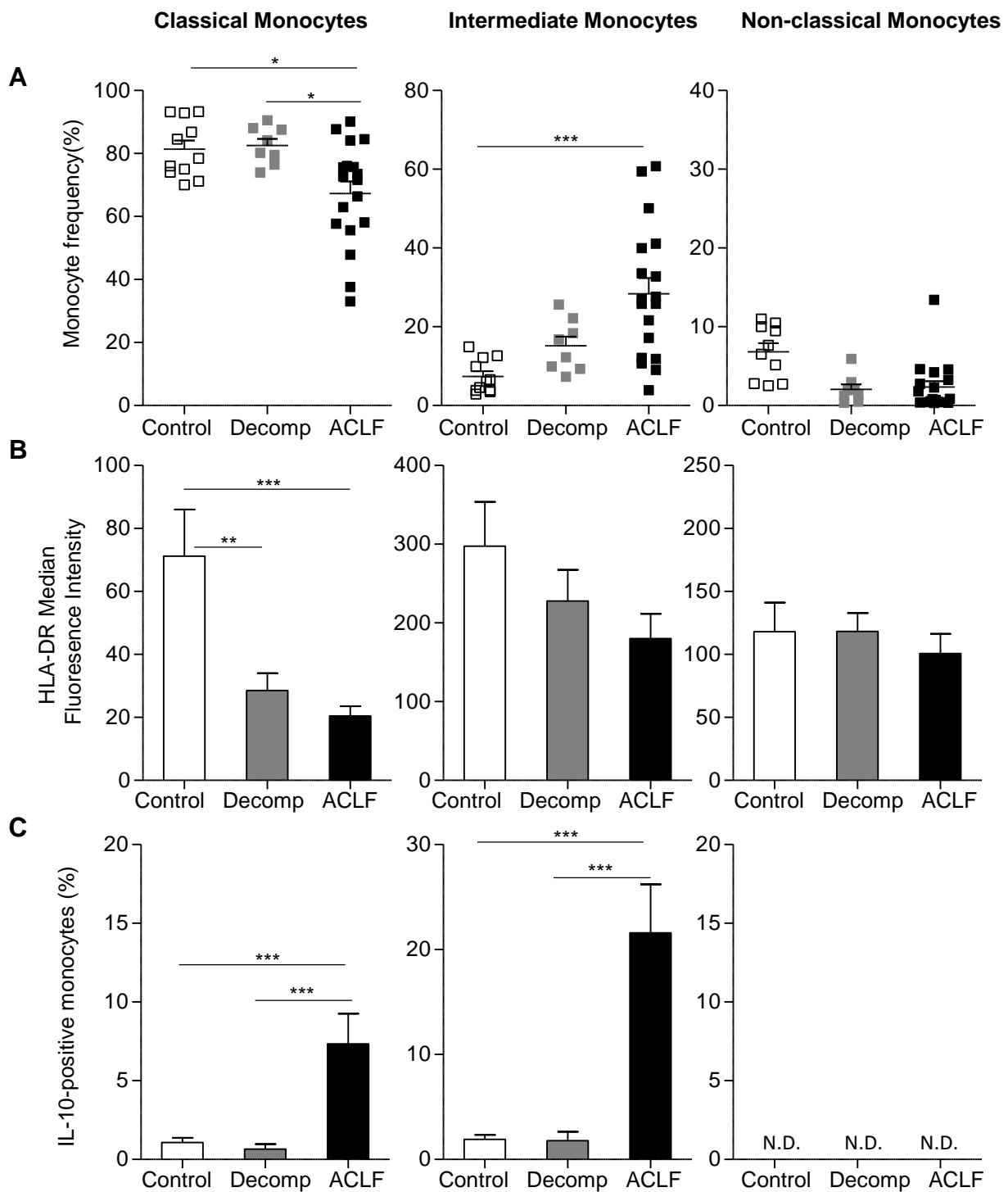
## References

- 1 Arroyo V, Moreau R, Kamath PS, *et al.* Acute-on-chronic liver failure in cirrhosis. *Nat Rev Dis Prim* 2016;**2**:16041. doi:10.1038/nrdp.2016.41
- 2 Katoonizadeh A, Laleman W, Verslype C, *et al.* Early features of acute-on-chronic alcoholic liver failure: a prospective cohort study. *Gut* 2010;**59**:1561–9. doi:10.1136/gut.2009.189639
- 3 Arroyo V, Moreau R, Jalan R, *et al.* Acute-on-chronic liver failure: A new syndrome that will re-classify cirrhosis. *J Hepatol* 2015;**62**:S131–43. doi:10.1016/j.jhep.2014.11.045
- 4 Moreau R, Jalan R, Gines P, *et al.* Acute-on-Chronic Liver Failure Is a Distinct Syndrome That Develops in Patients With Acute Decompensation of Cirrhosis. *Gastroenterology* 2013;**144**:1426–1437.e9. doi:10.1053/j.gastro.2013.02.042
- 5 Laleman W, Verbeke L, Meersseman P, *et al.* Acute-on-chronic liver failure: current concepts on definition, pathogenesis, clinical manifestations and potential therapeutic interventions. *Expert Rev Gastroenterol Hepatol* 2011;**5**:523–37. doi:10.1586/egh.11.47
- 6 Meersseman P, Langouche L, du Plessis J, *et al.* The Intensive Care Unit (ICU) course and outcome in Acute-on-chronic liver failure are comparable to other populations. *J Hepatol* 2018;**0**. doi:10.1016/j.jhep.2018.04.025
- 7 Moreau R, Arroyo V. Acute-on-Chronic Liver Failure: A New Clinical Entity. *Clin Gastroenterol Hepatol* 2015;**13**:836–41. doi:10.1016/j.cgh.2014.02.027
- 8 Tandon P, Garcia-Tsao G. Bacterial Infections, Sepsis, and Multiorgan Failure in Cirrhosis. *Semin Liver Dis* 2008;**28**:026–42. doi:10.1055/s-2008-1040319
- 9 Albillos A, Lario M, Álvarez-Mon M. Cirrhosis-associated immune dysfunction: Distinctive features and clinical relevance. *J Hepatol* 2014;**61**:1385–96. doi:10.1016/j.jhep.2014.08.010
- 10 Clària J, Arroyo V, Moreau R. The Acute-on-Chronic Liver Failure Syndrome, or When the Innate Immune System Goes Astray. *J Immunol* 2016;**197**:3755–61. doi:10.4049/jimmunol.1600818
- 11 Ginhoux F, Jung S. Monocytes and macrophages: developmental pathways and tissue homeostasis. *Nat Rev Immunol* 2014;**14**:392–404. doi:10.1038/nri3671
- 12 Blander JM, Sander LE. Beyond pattern recognition: five immune checkpoints for scaling the microbial threat. *Nat Rev Immunol* 2012;**12**:215–25. doi:10.1038/nri3167
- 13 Taylor PR, Martinez-Pomares L, Stacey M, *et al.* MACROPHAGE RECEPTORS AND IMMUNE RECOGNITION. *Annu Rev Immunol* 2005;**23**:901–44. doi:10.1146/annurev.immunol.23.021704.115816

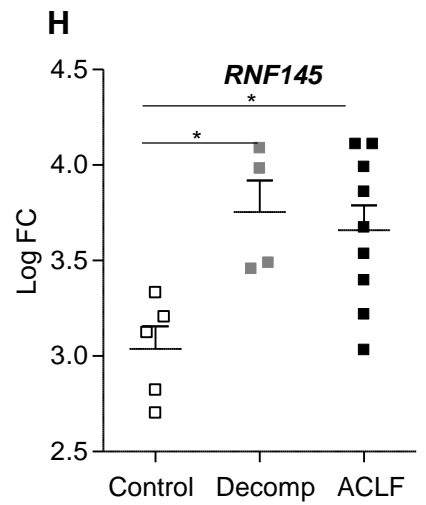
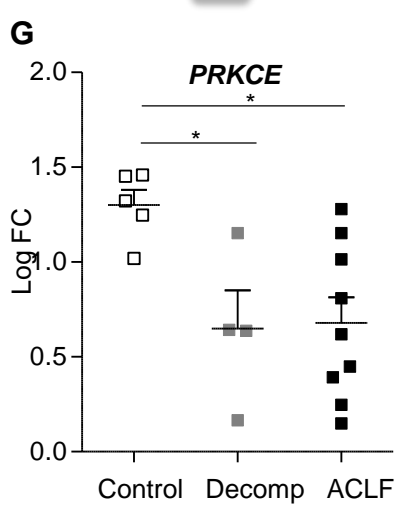
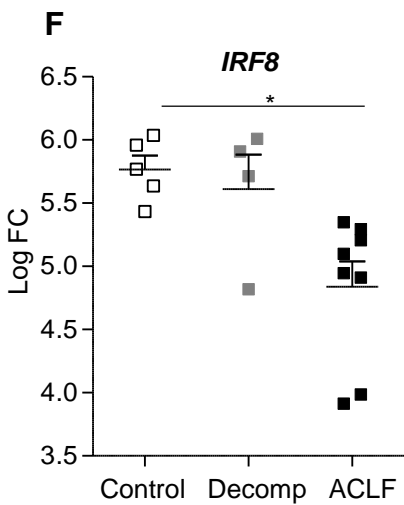
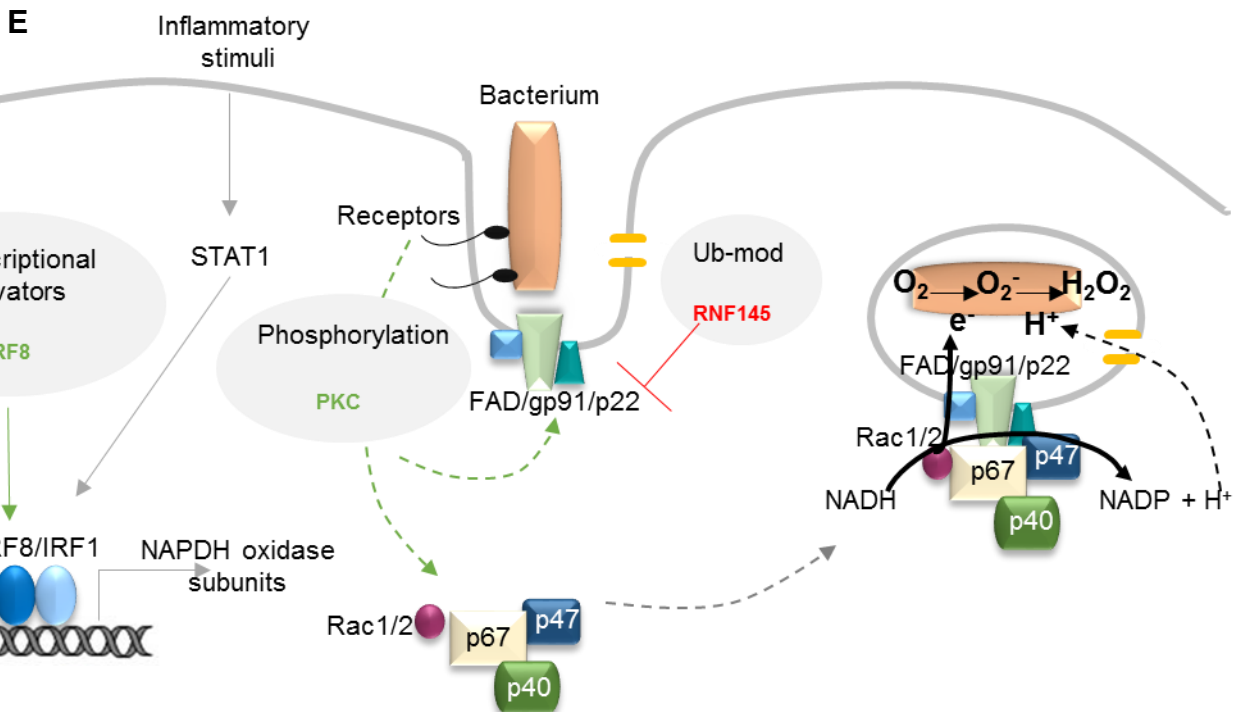
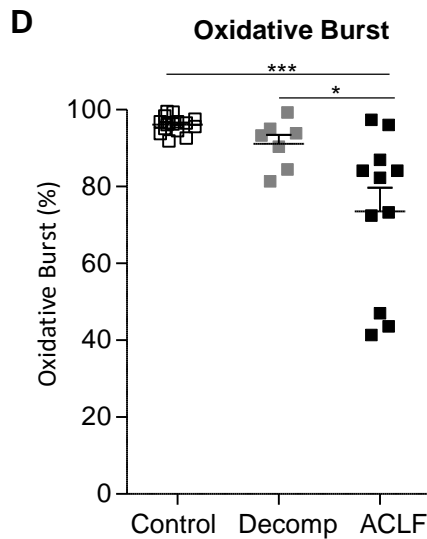
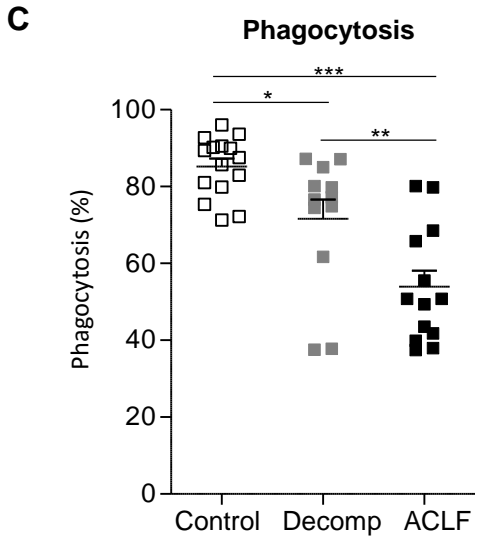
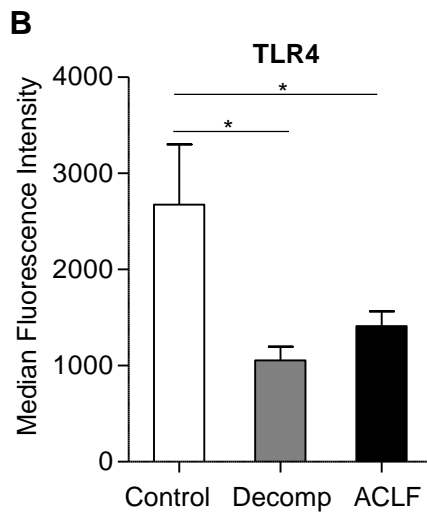
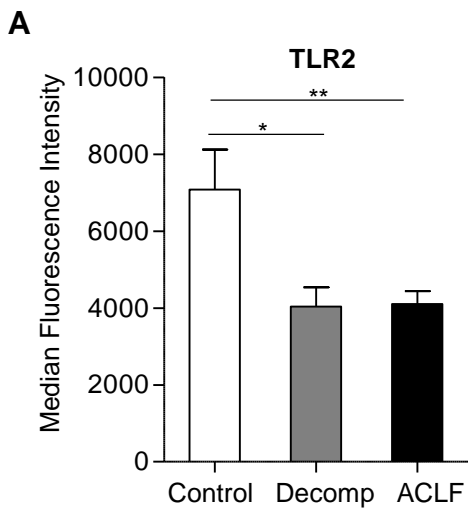
- 14 Biswas SK, Mantovani A. Macrophage plasticity and interaction with lymphocyte subsets: cancer as a paradigm. *Nat Immunol* 2010;**11**:889–96. doi:10.1038/ni.1937
- 15 Wynn TA, Chawla A, Pollard JW. Macrophage biology in development, homeostasis and disease. *Nature* 2013;**496**:445–55. doi:10.1038/nature12034
- 16 Shi Y, Wu W, Yang Y, *et al.* Decreased Tim-3 expression is associated with functional abnormalities of monocytes in decompensated cirrhosis without overt bacterial infection. *J Hepatol* 2015;**63**:60–7. doi:10.1016/j.jhep.2015.02.020
- 17 Antoniadou CG, Wendon J, Vergani D. Paralyzed monocytes in acute on chronic liver disease. doi:10.1016/j.jhep.2004.12.005
- 18 Bernsmeier C, Triantafyllou E, Brenig R, *et al.* CD14<sup>+</sup> CD15<sup>-</sup> HLA-DR<sup>-</sup> myeloid-derived suppressor cells impair antimicrobial responses in patients with acute-on-chronic liver failure. *Gut* Published Online First: 2017. doi:10.1136/gutjnl-2017-314184
- 19 O'Brien AJ, Fullerton JN, Massey KA, *et al.* Immunosuppression in acutely decompensated cirrhosis is mediated by prostaglandin E2. *Nat Med* Published Online First: 2014. doi:10.1038/nm.3516
- 20 McGettrick AF, O'Neill LAJ. How Metabolism Generates Signals during Innate Immunity and Inflammation. *J Biol Chem* 2013;**288**:22893–8. doi:10.1074/jbc.R113.486464
- 21 O'Neill LAJ, Hardie DG. Metabolism of inflammation limited by AMPK and pseudo-starvation. *Nature* 2013;**493**:346–55. doi:10.1038/nature11862
- 22 O'Neill LAJ, Pearce EJ. Immunometabolism governs dendritic cell and macrophage function. *J Exp Med* Published Online First: 2016. doi:10.1084/jem.20151570
- 23 Stanley IA, Ribeiro SM, Giménez-Cassina A, *et al.* Changing appetites: the adaptive advantages of fuel choice. *Trends Cell Biol* 2014;**24**:118–27. doi:10.1016/j.tcb.2013.07.010
- 24 Huang SC-C, Everts B, Ivanova Y, *et al.* Cell-intrinsic lysosomal lipolysis is essential for alternative activation of macrophages. *Nat Immunol* 2014;**15**:846–55. doi:10.1038/ni.2956
- 25 Jha AK, Huang SCC, Sergushichev A, *et al.* Network integration of parallel metabolic and transcriptional data reveals metabolic modules that regulate macrophage polarization. *Immunity* Published Online First: 2015. doi:10.1016/j.immuni.2015.02.005
- 26 Rodriguez-Prados J-C, Traves PG, Cuenca J, *et al.* Substrate Fate in Activated Macrophages: A Comparison between Innate, Classic, and Alternative Activation. *J Immunol* 2010;**185**:605–14. doi:10.4049/jimmunol.0901698

- 27 Biswas SK, Mantovani A. Orchestration of Metabolism by Macrophages. *Cell Metab* 2012;**15**:432–7. doi:10.1016/j.cmet.2011.11.013
- 28 Vats D, Mukundan L, Odegaard JI, *et al.* Oxidative metabolism and PGC-1 $\beta$  attenuate macrophage-mediated inflammation. *Cell Metab* 2006;**4**:13–24. doi:10.1016/j.cmet.2006.05.011
- 29 Abeles RD, McPhail MJ, Sowter D, *et al.* CD14, CD16 and HLA-DR reliably identifies human monocytes and their subsets in the context of pathologically reduced HLA-DR expression by CD14hi/CD16neg monocytes: Expansion of CD14hi/CD16pos and contraction of CD14lo/CD16pos monocytes in acute liver fail. *Cytom Part A* 2012;**81A**:823–34. doi:10.1002/cyto.a.22104
- 30 Heulens N, Korf H, Cielen N, *et al.* Vitamin D deficiency exacerbates COPD-like characteristics in the lungs of cigarette smoke-exposed mice. *Respir Res* 2015;**16**:110. doi:10.1186/s12931-015-0271-x
- 31 Bernsmeier C, Pop OT, Singanayagam A, *et al.* Patients with acute-on-chronic liver failure have increased numbers of regulatory immune cells expressing the receptor tyrosine kinase MERTK. *Gastroenterology* Published Online First: 2015. doi:10.1053/j.gastro.2014.11.045
- 32 Triantafyllou E, Pop OT, Possamai LA, *et al.* MerTK expressing hepatic macrophages promote the resolution of inflammation in acute liver failure. *Gut* 2018;**67**:333–47. doi:10.1136/gutjnl-2016-313615
- 33 O’Neill LAJ, Kishton RJ, Rathmell J. A guide to immunometabolism for immunologists. *Nat. Rev. Immunol.* 2016. doi:10.1038/nri.2016.70
- 34 Geeraerts X, Bolli E, Fendt SM, *et al.* Macrophage metabolism as therapeutic target for cancer, atherosclerosis, and obesity. *Front. Immunol.* 2017. doi:10.3389/fimmu.2017.00289
- 35 Wellen KE, Thompson CB. A two-way street: reciprocal regulation of metabolism and signalling. *Nat Rev Mol Cell Biol* 2012;**13**:270–6. doi:10.1038/nrm3305
- 36 Graham DB, Becker CE, Doan A, *et al.* Functional genomics identifies negative regulatory nodes controlling phagocyte oxidative burst. *Nat Commun* Published Online First: 2015. doi:10.1038/ncomms8838
- 37 Langlais D, Barreiro LB, Gros P. The macrophage IRF8/IRF1 regulome is required for protection against infections and is associated with chronic inflammation. *J Exp Med* Published Online First: 2016. doi:10.1084/jem.20151764
- 38 Chistiakov DA, Myasoedova VA, Revin V V., *et al.* The impact of interferon-regulatory

- factors to macrophage differentiation and polarization into M1 and M2. *Immunobiology* 2018;**223**:101–11. doi:10.1016/j.imbio.2017.10.005
- 39 Cheng SC, Scicluna BP, Arts RJW, *et al.* Broad defects in the energy metabolism of leukocytes underlie immunoparalysis in sepsis. *Nat Immunol* Published Online First: 2016. doi:10.1038/ni.3398
- 40 Pena OM, Pistolic J, Raj D, *et al.* Endotoxin Tolerance Represents a Distinctive State of Alternative Polarization (M2) in Human Mononuclear Cells. *J Immunol* 2011;**186**:7243–54. doi:10.4049/jimmunol.1001952
- 41 Shalova IN, Lim JY, Chittezhath M, *et al.* Human monocytes undergo functional re-programming during sepsis mediated by hypoxia-inducible factor-1 $\alpha$ . *Immunity* Published Online First: 2015. doi:10.1016/j.immuni.2015.02.001
- 42 Venet F, Monneret G. Advances in the understanding and treatment of sepsis-induced immunosuppression. *Nat Rev Nephrol* 2017;**14**:121–37. doi:10.1038/nrneph.2017.165
- 43 Wiest R, Lawson M, Geuking M. Pathological bacterial translocation in liver cirrhosis. *J Hepatol* 2014;**60**:197–209. doi:10.1016/j.jhep.2013.07.044
- 44 Schierwagen R, Alvarez-Silva C, Madsen MSA, *et al.* Circulating microbiome in blood of different circulatory compartments. *Gut* 2018;;gutjnl-2018-316227. doi:10.1136/gutjnl-2018-316227
- 45 Hackstein C-P, Assmus LM, Welz M, *et al.* Gut microbial translocation corrupts myeloid cell function to control bacterial infection during liver cirrhosis. *Gut* 2017;**66**:507–18. doi:10.1136/gutjnl-2015-311224
- 46 O’Neill LAJ. A Metabolic Roadblock in Inflammatory Macrophages. *Cell Rep.* 2016. doi:10.1016/j.celrep.2016.09.085
- 47 Jha AK, Huang SC-C, Sergushichev A, *et al.* Network Integration of Parallel Metabolic and Transcriptional Data Reveals Metabolic Modules that Regulate Macrophage Polarization. *Immunity* 2015;**42**:419–30. doi:10.1016/j.immuni.2015.02.005
- 48 Palmieri EM, Menga A, Martín-Pérez R, *et al.* Pharmacologic or Genetic Targeting of Glutamine Synthetase Skews Macrophages toward an M1-like Phenotype and Inhibits Tumor Metastasis. *Cell Rep* Published Online First: 2017. doi:10.1016/j.celrep.2017.07.054

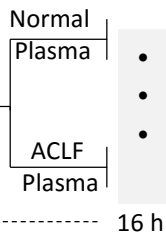






**A**

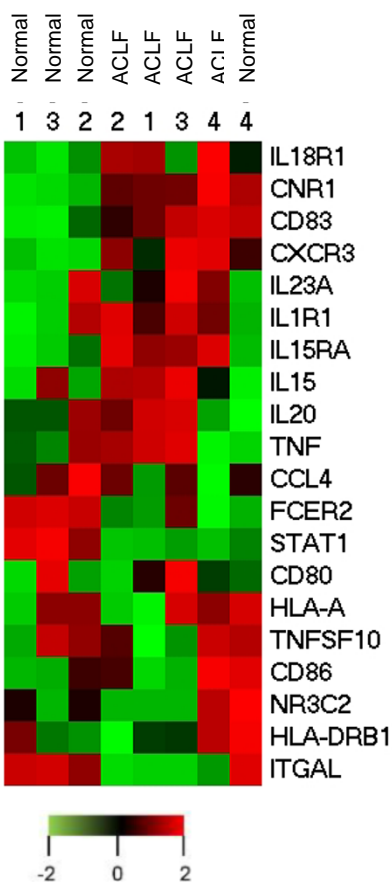
Healthy Donors  
CD14<sup>+</sup> Isolation



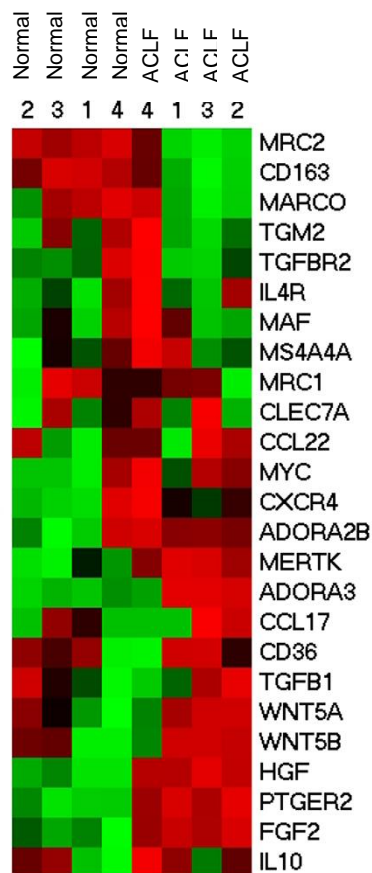
- RNAsequencing
- Cytokines
- Phagocytosis

**B**

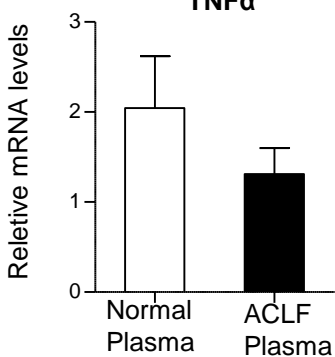
Proinflammatory

**C**

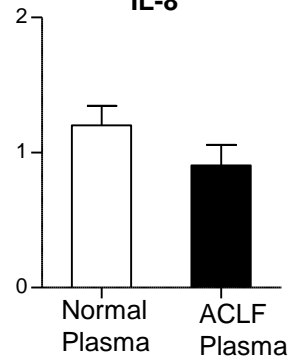
Anti-inflammatory

**D**

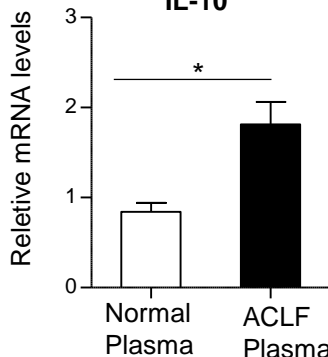
TNF $\alpha$



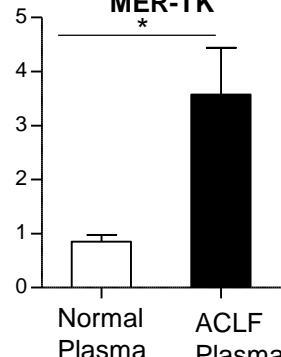
IL-8

**E**

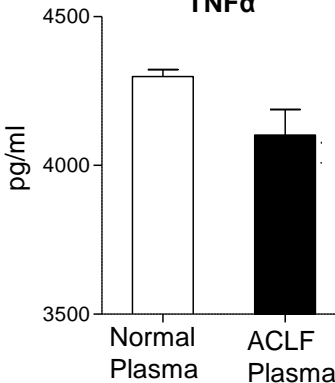
IL-10



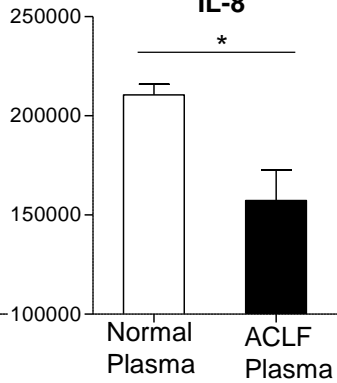
MER-TK

**F**

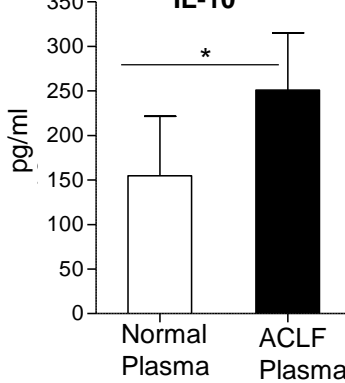
TNF $\alpha$



IL-8

**G**

IL-10

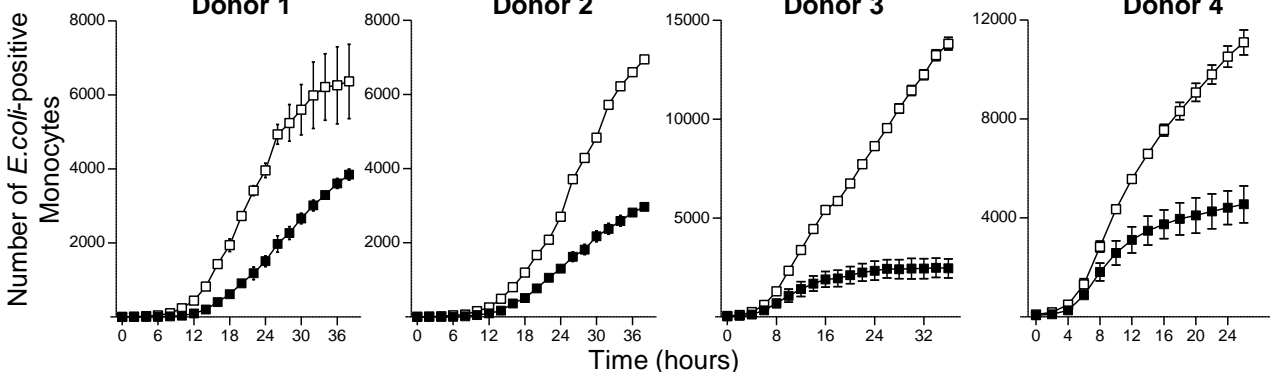
**H**

Donor 1

Donor 2

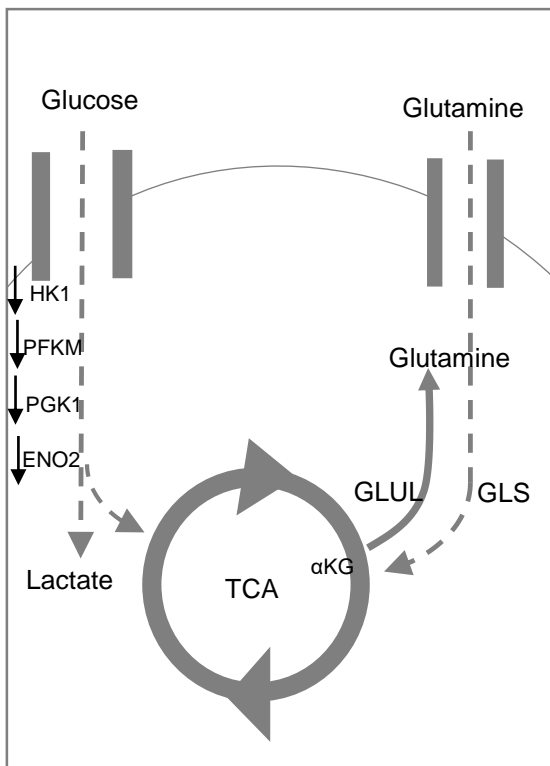
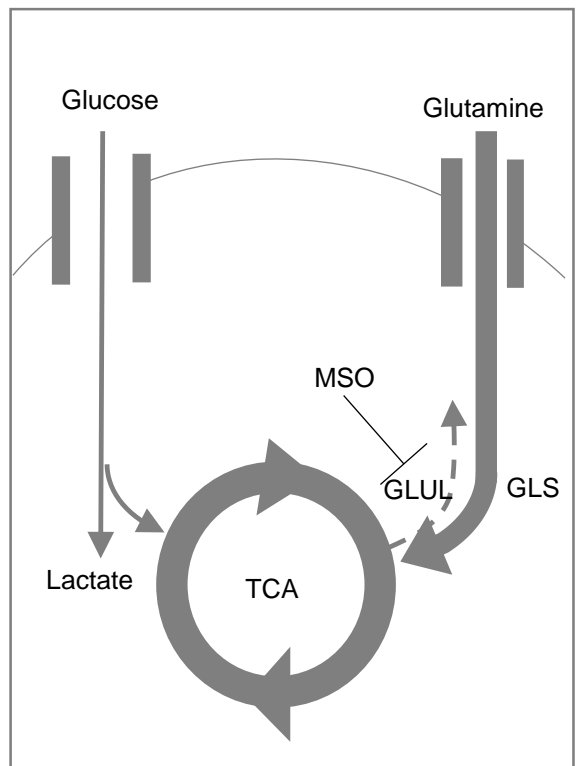
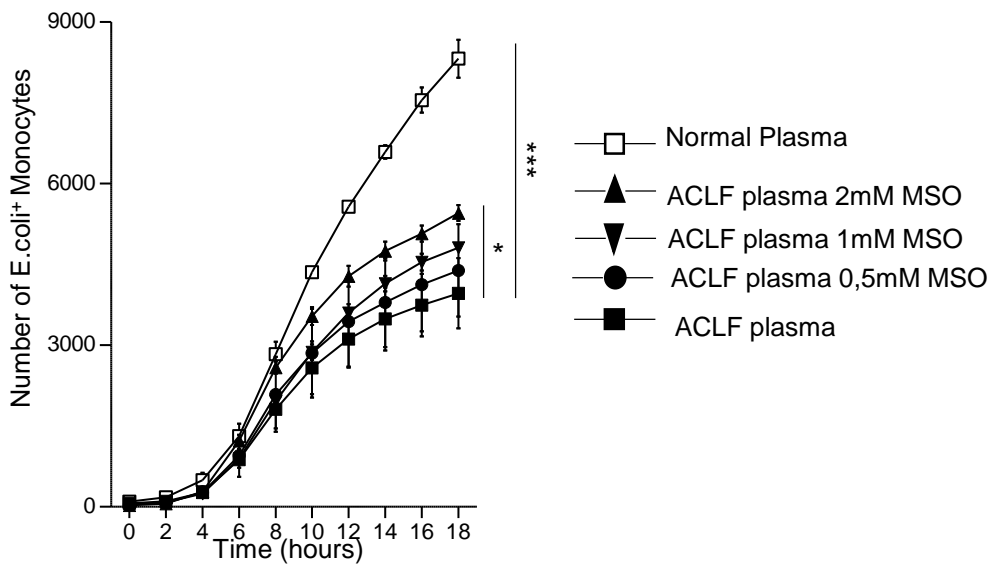
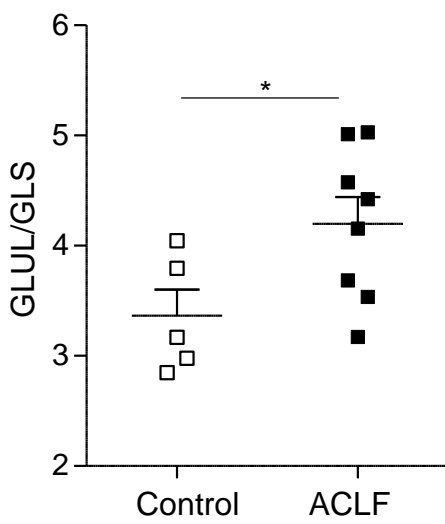
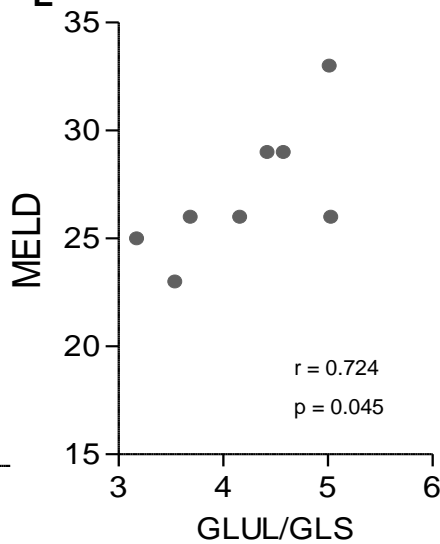
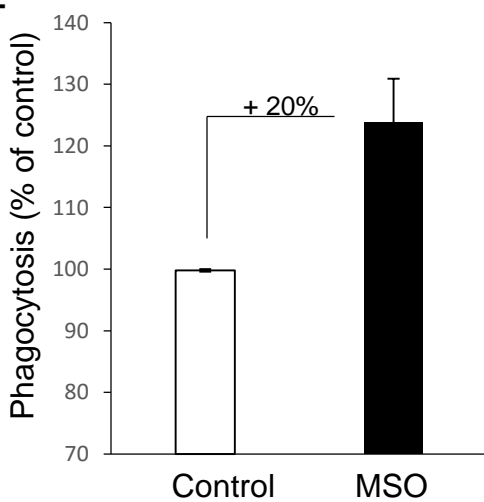
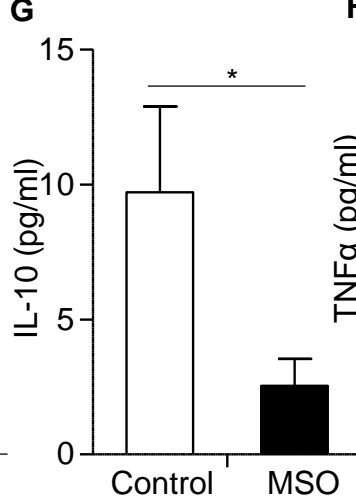
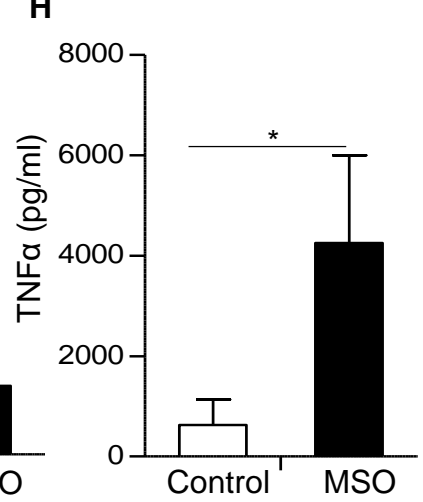
Donor 3

Donor 4



□ Normal Plasma

■ ACLF Plasma

**A****B****C****D****E****F****G****H**

**Inhibition of glutamine synthetase in monocytes from patients with Acute-on-Chronic Liver Failure partially resuscitates their antibacterial and inflammatory capacity**

**Short running title:** Reviving monocyte function in ACLF

Hannelie Korf<sup>1,†</sup>, Johannie du Plessis<sup>1,2</sup>, Jos van Pelt<sup>3</sup>, Sofie De Groote<sup>1</sup>, David Cassiman<sup>1,4</sup>, Len Verbeke<sup>1,4</sup>, Bart Ghesquière<sup>5</sup>, Sarah-Maria Fendt<sup>6,7</sup>, Matthew J Bird<sup>1,5</sup>, Ali Talebi<sup>8</sup>, Matthias Van Haele<sup>9</sup>, Rita Feio-Azevedo<sup>1</sup>, Lore Meelberghs<sup>1</sup>, Tania Roskams<sup>9</sup>, Raj Mookerjee<sup>10</sup>, Gautam Mehta<sup>10</sup>, Rajiv Jalan<sup>10</sup>, Thierry Gustot<sup>11</sup>, Wim Laleman<sup>1,4</sup>, Frederik Nevens<sup>1,4</sup>, Schalk van der Merwe<sup>1,4†</sup>

## Supplemental methods

### RNA isolation and qRT-PCR

RNA was isolated using Trizol (Thermo Fisher Scientific) and the RNeasy Mini Kit (Qiagen, Heidelberg, Germany) according to the manufacturer's instructions. RNA quantity and quality was measured using a NanoDrop spectrophotometer (NanoDrop Technologies, Wilmington, USA) and an Agilent 2100 bioanalyzer (Agilent Technologies, Santa Clara, USA). Samples meeting a RNA integrity number criterion of  $>8$  were used for subsequent studies. One microgram of cellular RNA was reverse transcribed into cDNA using SuperScript II reverse transcriptase and random hexamer primers (Invitrogen/Life Technologies, USA). The PCR reaction was carried out in a mixture that contained appropriate sense- and anti-sense primers and a TaqMan MGB probe in Taq-Man Universal PCR Master Mixture (Applied Biosystems, Foster City, USA). Beta-2-microglobulin was used as housekeeping gene. qRT-PCR amplification and data analysis was performed using the Lightcycler 96 (Roche Applied Science, Penzberg, Germany). Each sample was assayed in duplicate. The  $\Delta\Delta C_q$  method was used to determine relative gene expression levels.

### Next Generation Sequencing (NGS) and data processing

NGS was performed on isolated CD14<sup>+</sup> cells derived from ACLF patients and healthy controls or from CD14<sup>+</sup> cells modulated *in vitro* with ACLF plasma. Briefly, poly-A containing mRNA molecules were purified from the total RNA input using poly-T oligo-attached magnetic beads. Standard Illumina unstranded poly-A enriched libraries were prepared and sequencing thereof (paired-end 75 bp reads) occurred on an Illumina NextSeq 500 half flow cell to a depth of 4.1-7.1 million reads per sample (in quadruple). After preprocessing, reads were aligned with STAR 2.4.1d to the reference genome of Homo sapiens (GRCh37.73) and counted with featureCounts 1.4.6 (1, 2). With the EdgeR 3.8.6 package of Bioconductor (3), generalized linear model (GLM) was fitted against the normalized counts (4).

### Data analysis

To identify the differentially expressed genes between CD14<sup>+</sup> cells of ACLF patients compared to healthy controls, **unpaired analysis** was performed. To identify significantly changed gene expression in isolated CD14<sup>+</sup> cells that were cultured in the presence of serum we performed **paired analysis**. The individual results were combined, the average computed and the resulting p-values of the Limma and EdgeR packages were corrected for multiple testing with Benjamini–Hochberg to control false discovery rate for paired and unpaired analysis (5). A gene was considered differentially expressed if a 2log fold change  $>+1$  or  $<-1$  and a corrected  $p < 0.05$ . We used this *in silico* analysis to investigate the biological processes and KEGG pathways involved in ACLF. The genes differentially expressed in one direction in patients or after *in vitro* modulation were used as input in the software packet Webgestalt (<http://www.webgestalt.org/>). This program is designed for functional genomic, proteomic and large-scale genetic studies. The software proposes, based on strict statistical testing, likely functional

networks, including: 1) GO (geneontology) **Biological Process** that are defined as operations or sets of molecular events with a defined beginning and end, pertinent to the functioning of integrated living units: cells, tissues, organs, and organisms (<http://geneontology.org/>) and 2) **KEGG PATHWAYS**, which is a collection of manually drawn pathway maps representing our knowledge on the molecular interaction and reaction networks (<http://www.genome.jp/kegg/pathway.html>). Additional analysis of molecular interactions was done using STRING 10.0 algorithmic, a software that can predict interactions based on literature and other electronic information. The program visualizes reported gene interactions whereby the lines indicate the strength of association (6). Notably, because the number of genes is mostly a fraction of all the genes assigned to a specific KEGG pathway, computer analysis can map the same gene sets to different molecular processes (having mutual genes but different function). Notwithstanding, further evaluation and **data interpretation** by the researcher is always required to allow integration with the biological setup. Further of importance is that we applied **paired analysis** in order to compensating for the biological differences that exists between individual healthy donors (natural variation present already at the time of monocyte isolation). Notably, with the **hierarchic cluster analysis** of *in vitro* gene expression this biological variation could not be compensated for in the same way as in paired analysis.

**Supplemental Table 1: Clinical characteristics of patients admitted with decompensated cirrhosis and ACLF**

| Clinical parameter                     | Decompensated cirrhosis (n=19) | ACLF (n=22)    | p-value |
|--|--------------------------------|----------------|---------|
| Age (yrs)                              | 59 [46-68]                     | 54 [49-61]     | ns      |
| Gender, Male (%)                       | (10(53%))                      | (12(55%))      | ns      |
| Total bilirubin (mg/dl)                | 3 [2-5]†                       | 15 [11-26]†    | p<0.001 |
| ALT (U/L)                              | 26 [16-43]†                    | 42 [30-82]†    | p=0.002 |
| AST (U/L)                              | 56 [29-85]†                    | 98 [61-220]†   | p<0.001 |
| ALP (U/L)                              | 109 [91-162]                   | 136 [122-188]  | p=0.002 |
| GGT (U/L)                              | 70 [24-157]                    | 106 [56-245]   | p<0.001 |
| Albumin (g/dl)                         | 32 [26-34]                     | 28 [25-32]     | ns      |
| Creatinine (mg/dl)                     | 1.0 [0.8-1.6]                  | 1.2 [0.8-1.7]  | p=0.008 |
| Platelet count (x10 <sup>9</sup> /L)   | 143 [88-188]†                  | 83 [57-127]†   | p=0.01  |
| INR                                    | 1.6 [1.3-2.3]†                 | 2.3 [2.1-2.8]† | p<0.001 |
| MELD                                   | 16 [9-24]†                     | 28 [22-35]†    | p<0.001 |
| Child-Pugh                             | 10 [8-12]†                     | 12 [11-12]†    | p<0.001 |
| Maddrey                                | 20 [14-59]†                    | 83 [66-115]†   | p<0.001 |
| CLIF ACLF (1,2,3)                      | -                              | (9/12/1)       |         |
| Ascites (n(%))                         | (19(100%))                     | (18(82%))      | p<0.001 |
| Encephalopathy (n(%))                  | (10(53%))                      | (15(68%))      | p=0.002 |
| Renal failure (n(%))                   | (7(37%))                       | (9(40%))       | p=0.03  |
| White cell count (x10 <sup>9</sup> /L) | 7 [5-10]                       | 10 [7-14]      | p=0.03  |
| CRP (mg/L)                             | 13 [8-37]                      | 33 [16-46]     | ns      |
| Blood culture positive (n(%))          | (2(11%))                       | (8(36%))       | ns      |
| Urine culture positive (n(%))          | (3(16%))                       | (1(5%))        | ns      |
| Infiltrates on chest X-ray (n(%))      | (1(5%))†                       | (11(50%))†     | p=0.002 |
| Antibiotic treatment (n(%))            | (11(58%))                      | (19(86%))      | p<0.001 |
| Steroid treatment (n(%))               | (0(0%))†                       | (14(64%))†     | p<0.001 |
| 30-day mortality (n(%))                | (0(0%))†                       | (5(23%))†      | p=0.007 |
| Admitted to ICU (n(%))                 | (6(32%))                       | (13(59%))      | p=0.005 |

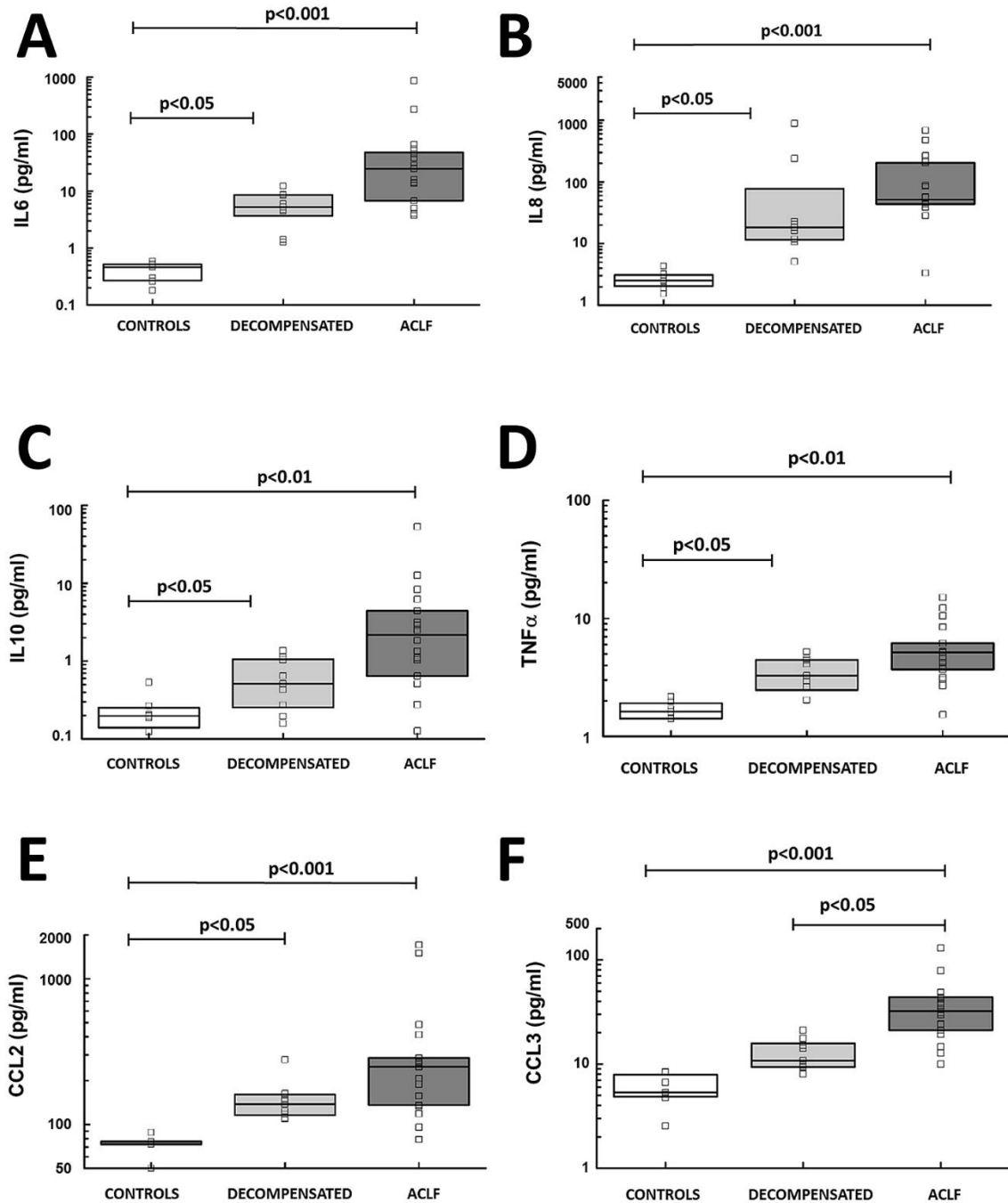
Data are presented as mean±SEM, median [IQR] or number of patients (%).†Decompensated vs ACLF p<0.05.

**Supplemental Table 2: Clinical characteristics of patients included for monocyte transcriptional and functional analysis**

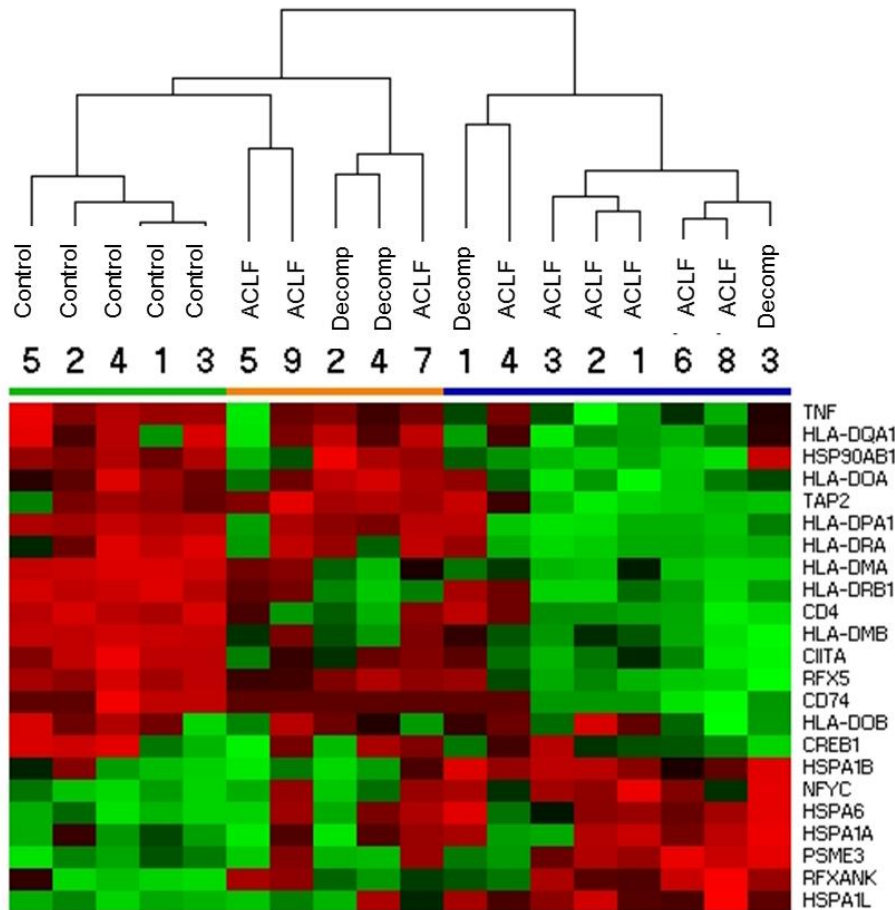
| Clinical parameter                     | Decompensated cirrhosis (n=4) | ACLF grade 2 (n=13) | p-value |
|--|-------------------------------|---------------------|---------|
| Age (yrs)                              | 66 [55-69]                    | 57 [53-61]          | ns      |
| Gender, Male (%)                       | (3(75%))                      | (10(77%))           | ns      |
| Total bilirubin (mg/dl)                | 5 [4-5]                       | 17 [10-23]          | p=0.002 |
| ALT (U/L)                              | 21 [17-24]                    | 47 [23-73]          | p=0.05  |
| AST (U/L)                              | 43 [27-65]                    | 124 [41-202]        | p=0.04  |
| ALP (U/L)                              | 119 [77-267]                  | 121 [106-192]       | ns      |
| GGT (U/L)                              | 127 [16-635]                  | 91 [30-264]         | ns      |
| Albumin (g/dl)                         | 29 [27-32]                    | 30 [23-36]          | ns      |
| Creatinine (mg/dl)                     | 0.7 [0.6-1.0]                 | 0.9 [0.7-1.5]       | ns      |
| Platelet count (x10 <sup>9</sup> /L)   | 82 [59-343]                   | 93 [64-157]         | ns      |
| INR                                    | 1.9 [1.2-2.7]                 | 2.6 [2.0-3.0]       | ns      |
| MELD                                   | 15 [11-25]                    | 29 [24-32]          | p<0.001 |
| Maddrey                                | 27                            | 75 [56-147]         | -       |
| Ascites (n(%))                         | (4(100%))                     | (11(84%))           | -       |
| Encephalopathy (n(%))                  | (3(75%))                      | (8(62%))            | ns      |
| Renal dysfunction (n(%))               | (0(0%))                       | (6(46%))            | -       |
| White cell count (x10 <sup>9</sup> /L) | 6 [4-7]                       | 8 [7-11]            | ns      |
| CRP (mg/L)                             | 11 [4-30]                     | 24 [10-38]          | ns      |
| Blood culture positive (n(%))          | -                             | (2(15%))            | -       |
| Antibiotic treatment (n(%))            | (0(0%))                       | (0(0%))             | -       |
| Steroid treatment (n(%))               | (0(0%))†                      | (0(0%))†            | -       |
| 30-day mortality (n(%))                | (0(0%))†                      | (10(77%))†          | -       |

Data are presented as mean±SEM, median [IQR] or number of patients (%).†ACLF vs Decompensated p<0.05

**Supplementary Figure 1: Quantification of circulating cytokines and chemokines in patients with alcoholic liver disease.** Cytokines and chemokines were measured in plasma samples collected from patients with ACLF (n=18), decompensated liver disease (n=9) and healthy controls (n=7) using MSDmesoscale multiplex immunoassays. The results are displayed as Median and IQR ( $p > 0.05$  was considered significant).

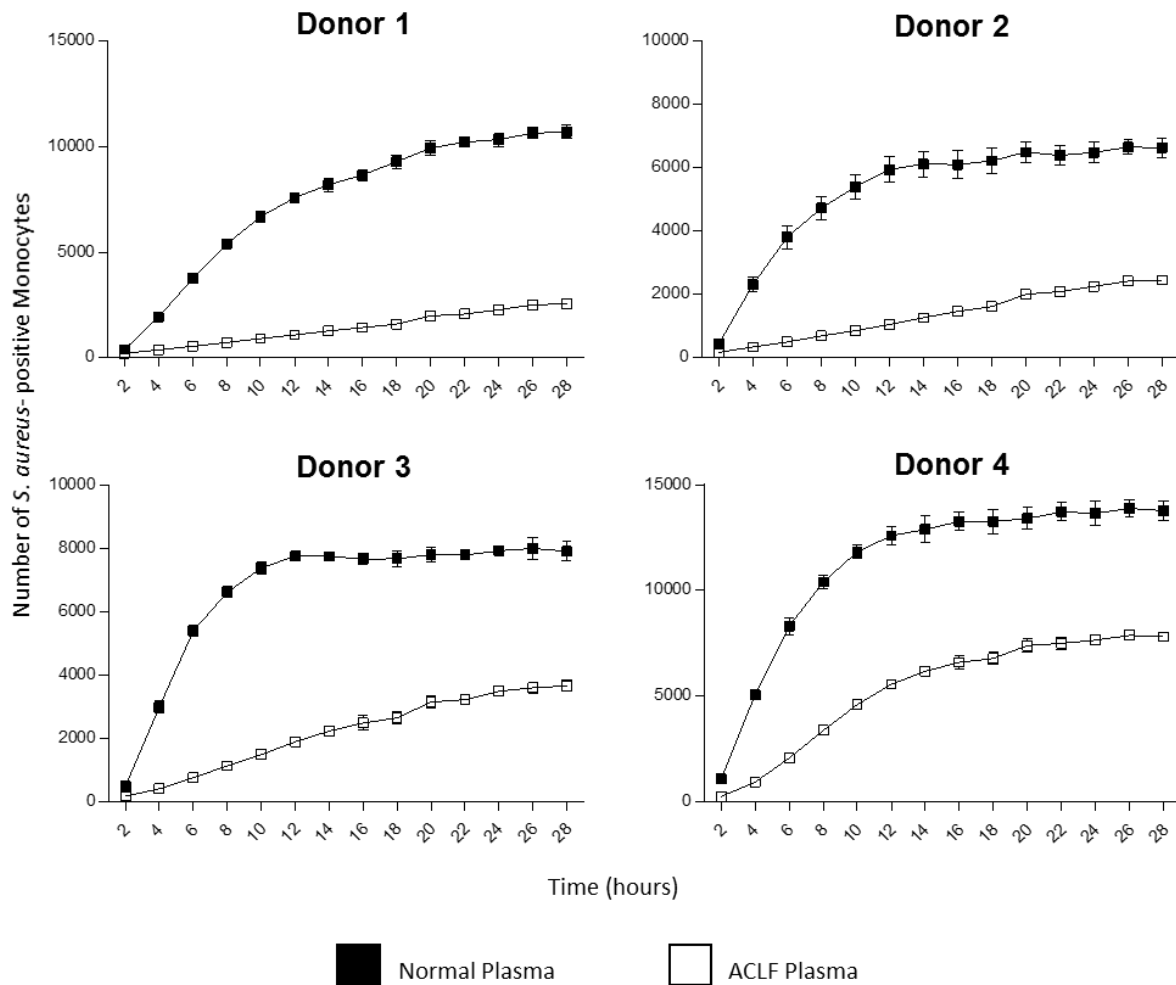


**Supplementary Figure 2:** Hierarchic clustering of gene expression of KEGG pathway hsa04612: antigen processing and presentation. Monocytes were isolated from control patients (n=5), Decomp (n=4) and ACLF (n=9) and NGS was performed. Clustering of pathway assigned genes resulted in 3 major groups as indicated by different color (blue, orange and green).

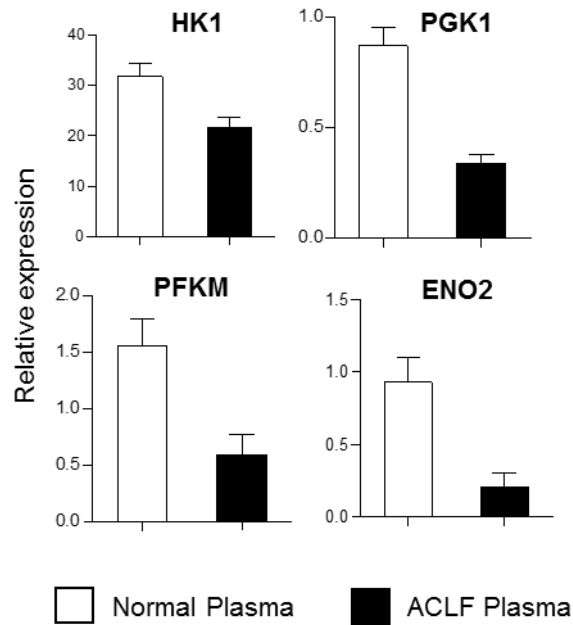




**Supplementary Figure 4:** Monocytes from four different healthy donors were cultured in the presence of ACLF or normal plasma (20% v/v) and challenged with pHrodo-labeled *S. aureus* at a previously optimized host:bacterium ratio. The frequency of monocytes that engulfed the bioparticles was evaluated using the IncuCyte system over a period of 24 hours.



**Supplementary Figure 5:** Quantification of key metabolic parameters from monocytes of healthy donors. Isolated CD14<sup>+</sup> monocytes were cultured in the presence or absence of ACLF plasma for 16 hours as described in the methods section. Relative mRNA levels of or metabolic parameters were determined by means of RT-qPCR at the end of the culture period. (Mean  $\pm$  SEM; n = 6).



## References

1. Dobin A, Davis CA, Schlesinger F, Drenkow J, Zaleski C, Jha S, Batut P, Chaisson M, Gingeras TR. STAR: ultrafast universal RNA-seq aligner. *Bioinformatics*. 2013;29(1):15-21.
2. Liao Y, Smyth GK, Shi W. featureCounts: an efficient general purpose program for assigning sequence reads to genomic features. *Bioinformatics*. 2014;30(7):923-30.
3. Gentleman RC, Carey VJ, Bates DM, Bolstad B, Dettling M, Dudoit S, Ellis B, Gautier L, Ge Y, Gentry J, Hornik K, Hothorn T, Huber W, Iacus S, Irizarry R, Leisch F, Li C, Maechler M, Rossini AJ, Sawitzki G, Smith C, Smyth G, Tierney L, Yang JY, Zhang J. Bioconductor: open software development for computational biology and bioinformatics. *Genome Biol*. 2004;5(10):R80.
4. Robinson MD, Smyth GK. Moderated statistical tests for assessing differences in tag abundance. *Bioinformatics*. 2007;23(21):2881-7.
5. Benjamini Y, Hochberg Y. Controlling the false discovery rate: a practical and powerful approach to multiple testing. *Journal of the Royal Statistical Society: Series B*. 1995;57:289-300.
6. Szklarczyk D, Franceschini A, Wyder S, Forslund K, Heller D, Huerta-Cepas J, Simonovic M, Roth A, Santos A, Tsafou KP, Kuhn M, Bork P, Jensen LJ, von Mering C. STRING v10: protein-protein interaction networks, integrated over the tree of life. *Nucleic Acids Res*. 2015 Jan; 43:D447-52.
7. Kondrup J, Allison SP, Elia M, Vellas B, Plauth M; Educational and Clinical Practice Committee, European Society of Parenteral and Enteral Nutrition (ESPEN).. ESPEN guidelines for nutrition screening 2002. *Clin Nutr*. 2003 Aug;22(4):415-21.
8. Vincent JL. New therapeutic implications of anticoagulation mediator replacement in sepsis and acute respiratory distress syndrome. *Crit Care Med*. 2000 Sep;28(9 Suppl):S83-5.